

# Final Project: Optimization of a pimple/dimple pattern on a flat plate

John Doe - Carmen Sandiego

University of Genoa, Course of Turbulence and CFD models, Course of Computational Optimization in Fluid Dynamics — September 2, 2020

## 1 Introduction

The aim of this study is to understand the basic principles that make pimples or dimpled surfaces able to reduce aerodynamic drag. The following RANS computation are part of a major study aimed at optimizing a pimple/dimple pattern on a Ahmed body to get a proper reduction in drag at the upper diffuser, where great part of the pressure-drag is generated as boundary-layer detachment occurs. The complete problem of the Ahmed body with these devices mounted was divided into simpler problems in which a fast optimization loop is possible using ANSYS tools: the complete Ahmed body is indeed too computationally expensive for a large set of accurate computations and it is difficult to see the effect of some basic parameters of the problem, as the flux around this geometry shows some complex features (vortices near the diffuser, horseshoe vortices near the "feet", BL detachment and relative unsteadiness...). For this reason a flat plate with an elementary set of pimples/dimples was considered first, to go, with increasing complexity, to a diffuser duct with a pattern of pimples/dimples with dimensions optimized using the previous loop and then, using these data, get a better starting point for the complete Ahmed body problem.

## 2 Choice of the turbulence model

The turbulence model chosen for the computations are two: for the 2D case the  $k-\omega$  SST model with the Kato-Launder production limiter was chosen; it wasn't added the curvature correction because it caused a reduction of the wall shear stress component along the whole plate and not a variation limited to the pimple or dimple region. This model was chosen because it is wall insensitive and in our application a wall resolving approach was desired (issue that can be handled by this model). In a second moment also a transition SST model [1] was used to understand how the pimple made the drag vary as a function of its positioning with respect to the transition point.

For the 3D case the  $k-\omega$  SST model was chosen, but for that case the curvature correction [2] was added (to account for the concentrated vortices generated by pimples and dimples) as well as the default production limiter (to account for stagnation points). Then the  $k-\omega$  SST model is also implemented in Fluent-Adjoint Solver with frozen turbulence [3].

### 3 Computational resources

The computational resources for the following simulations are two laptops, one with 4 cores INTEL i-7 7700HQ 2.8GHz and 16 GB RAM and the other with 4 cores INTEL i7-8550U 1.8GHz and 8GB RAM. Both of them have 64-bit architecture and SSD storage. The two resources were respectively dedicated to 3D and 2D computations mainly, taking into account their different attitudes.

### 4 Part 1: Preliminary computations on a 2D flat plate

The 2D case was chosen not only to have an idea of what could happen on a flat plate when a dimple or a pimple was added, but also because if some correlations were found between the 2D and the 3D case, it could represent an easier and faster way to obtain some results instead of running a full 3D case.

In the 2D case, 6 different experimental setups were run:

- single pimple setup;
- single dimple setup;
- double pimple setup;
- double dimple setup;
- a pimple followed by a dimple;
- a dimple followed by a pimple.

For each one of those setups a design of experiment (DOE) was made and a response surface model (RSM) was built to find if there were correlations between the different parameters.

**The flat plate at  $Re=250000$  shows a Drag of 0.13206 N, and at  $Re=1000000$  Drag becomes 1.56 N and the  $C_D = 0.0039$ . Those values will be used as a reference to evaluate the goodness of the different geometries.**

## 4.1 Geometry and mesh

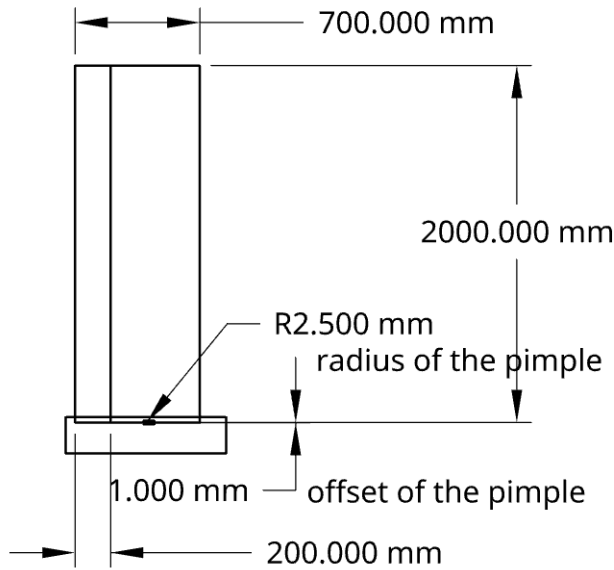


**Figure 1:** *Geometry for the pimple case.*

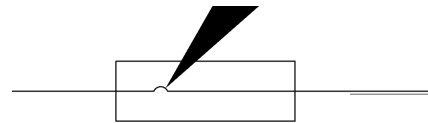


**Figure 2:** *Here it can be seen a focus of the geometry close to the pimple.*

For the 2D case, the domain had the following characteristics: it is rectangular, 2 meters tall and 0.5 meters long; then two bodies of influence were added to have a better resolution close to the pimple/dimple.

That height was chosen to avoid any influence from the top of the domain (that is a wall with no shear stress). The pimple/dimple is at 0.2 meters from the beginning of the flat plate, and it is parameterized to be able to vary its diameter and offset (distance between the center of the circle and the flat plate). The geometry of the pimple case can be seen in Fig.2; for the dimple case is the same but instead of a pimple there's a dimple.

A line was added to divide the domain in two sections: the first with the "symmetry" boundary condition and the second with the wall's one.

For the meshing it was chosen an "all triangles method", and were added sizings to the two bodies of influence (boi) and to the wall; the finest boi has an element size of 0.0008m, while the other is 0.002m. Those choices were made not to have a too strong difference of the mesh size between the bodies of influence, that could induce in diffusion errors. The domain element size is 0.05m while the edge sizing is 0.0005m with curvature capture enabled with  $2^\circ$  of curvature normal angle and a local refinement of 0.0001m. The named selections applied to the different parts of the mesh can be seen in figure 3.

## 4.2 First Setup

A first set of experiments was run at  $Re=250000$ , and the geometries that were used are:

1. single pimple with:
  - diameter in the range 0.001-0.005m;
  - offset in the range 0-0.00025m.

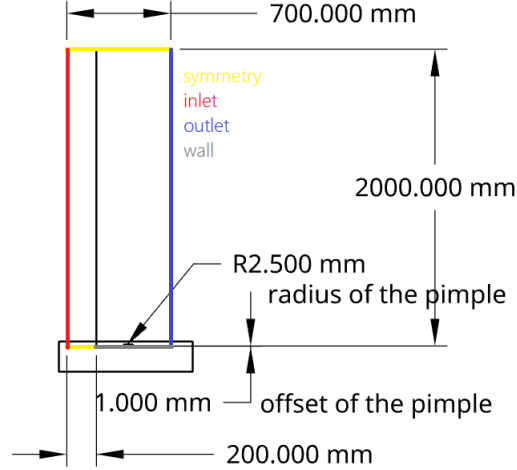


**Figure 3:** *Boundary conditions applied to the mesh.*

2. single dimple with:
  - diameter in the range 0.001-0.005m;
  - offset in the range 0-0.00025m.
3. double pimple;
4. double dimple;
5. pimple dimple;
6. dimple pimple.

To obtain that Reynolds number, and considering the incompressible flow, it was chosen:

- $\rho = 1kg/m^3$ ;
- $\mu = 2 \cdot 10^{-5}kg/ms$ ;
- $v = 10m/s$ ;
- $l = 0.5m$

The chosen turbulence model is the k- $\omega$  SST with Kato Launder production limiter; curvature correction wasn't enabled because it produced some unreal results: the shear stress was constantly lower than the one from the flat plate and this was not realistic. The chosen solution method is the COUPLED, that guarantees a fast convergence and due to the fact that this is a 2D case and it's not too heavy, it is also quite fast. The accuracy was set to second order at least for all the parameters and the under relaxation factors weren't changed because there were no oscillating behaviours that needed to be smoothed. Monitors for  $y_{average}^+$  and  $y_{maximum}^+$  were added and in all the cases those values were in the range between 1 and 0.1.

## 4.3 Results for Re=250000

### 4.3.1 Pimple

An RSM was built and that showed a smooth behaviour and, once saved the chart results on a post-processing program, it was possible to find out that it seems that exists a correlation that joins the diameter and the offset to the drag. In the 2D case it seems that the drag is only function of how high is the blockage, as it can be seen in Fig.4; so a simple correlation was found between the drag and the height of the "blockage" (eq. 1 ) which, on his hand, has also a simple equation 2:

$$drag = 73.6244 \cdot b^2 + 0.3968 \cdot b + 0.0036 \quad (1)$$

$$blockage = \frac{diameter_{pimple}}{2} - offset_{pimple}, \quad (2)$$

This equation was found using a second order least square regression and confirms the results found in 3D.

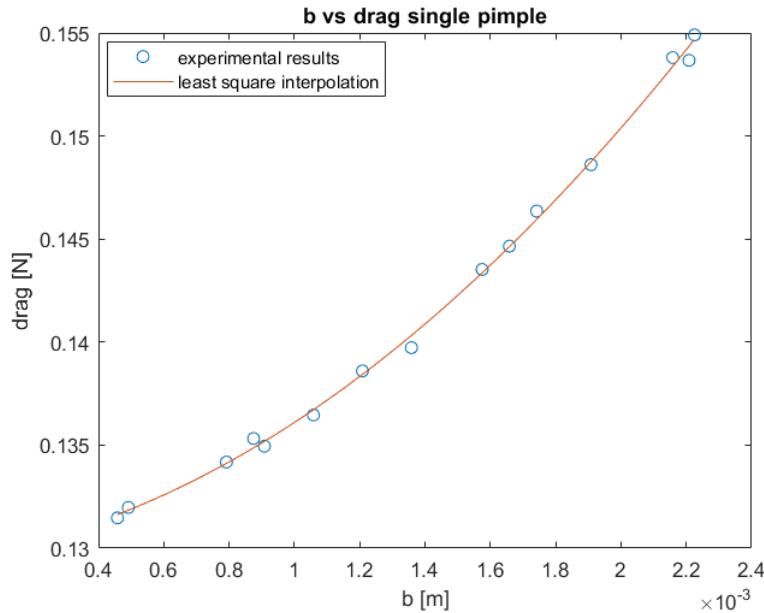


**Figure 4:** Correlation of  $b$  and Drag for the single pimple at Re 250000, with the least square regression.

From this RSM came out that the configuration with diameter of 0.00113m and offset of 0.000108m shows a lower drag than the flat plate equal to 0.1314 N, but this results could be wrong because of the small dimensions of the objects considered and the consequent mesh influence.

### 4.3.2 Dimple

Once done with the single pimple case, another DOE was made with a single dimple case and the results from the RSM were noisier and it was difficult to find a good correlation between  $b$  and the Drag, as it can be seen in Fig.5.

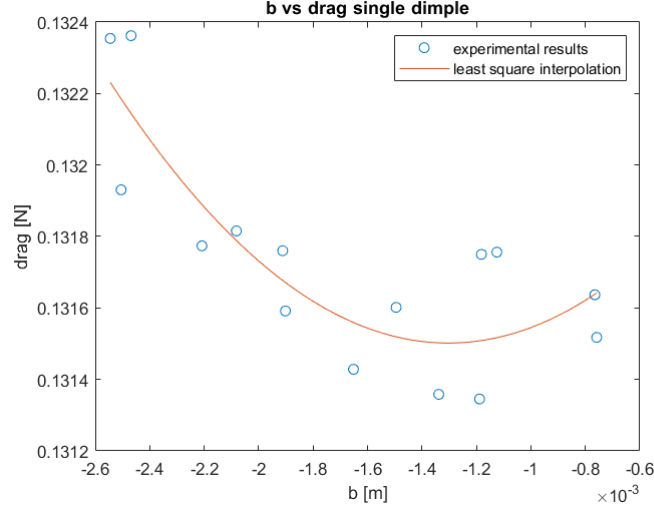


**Figure 5:** Correlation of  $b$  and Drag for the single dimple configuration.

Also, in this case a second order least square interpolation was used to fit the results of the DOE, but the function doesn't interpolate well the experimental values that are affected by too much noise.

From the RSM, it came out that the best configuration was the one obtained with a diameter of 0,0019565 m, an offset 1,0002 mm, that guarantee a drag of 0,13135 N. Also for the single dimple the result is very close to the flat plate case, so this result can't be considered significant.

#### 4.4 Results for $Re=1000000$

The calculations with such small geometries don't seem to have good results because they are too affected by uncertainty; so to have more accuracy (and less dependency on the mesh) for further investigations, bigger geometries were used and to get closer to what it can be obtained in a real application it was run at an higher Reynolds number.

For this case, that is more generalizable than the previous ones, data are presented using the Drag coefficient instead of the Drag force (eq.3).

$$C_D = \frac{D}{\frac{1}{2} \cdot \rho \cdot v^2 \cdot A}. \quad (3)$$

The Reynolds number is obtained changing only the velocity inlet, and keeping constant all the other parameters:

- $\rho = 1kg/m^3$ ;
- $\mu = 2 \cdot 10^{-5}kg/ms$ ;
- $v = 40m/s$ ;
- $l = 0.5m$

##### 4.4.1 "bigger" pimple

To find out if with bigger pimples there was an advantage, a DOE was run with the following ranges:

- diameter in the range 0.01 - 0.015m;
- offset in the range 0.002 - 0.004m;

and an RSM was built using the Kriging method and a set of 15 experimental points. With bigger pimples it was obtained a solution that is not affected by the small dimensions of the geometry; as expected the single pimple case increases the drag of the flat plate, the best solution is the one with the smallest blockage and for the ranges chosen it is obtained with a diameter of 0.01m and an offset of 0.001m that gives  $C_D = 0.0042$ . In the following figures it can be seen the RSM obtained with the Kriging (Fig.6) and the correlation between  $b$  and the drag (Fig.7) using eq.2.

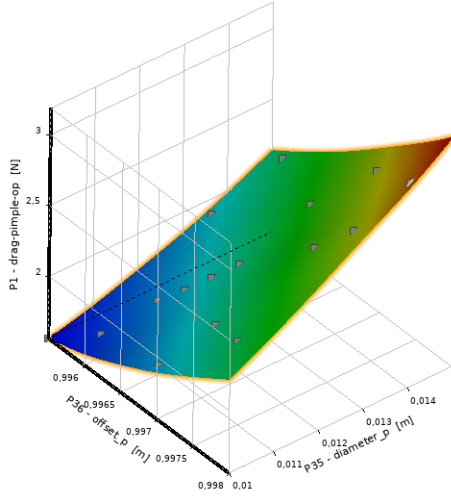


**Figure 6:** RSM of the single pimple configuration at  $Re\ 1000000$  using the Kriging method.

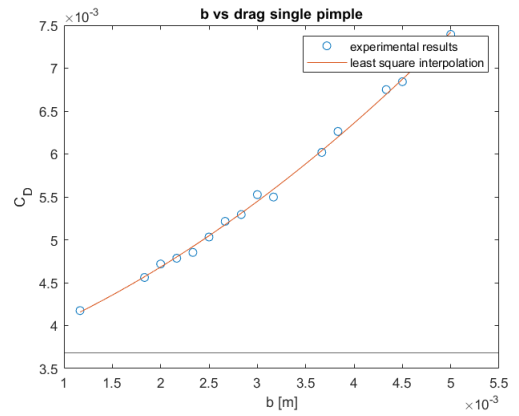


**Figure 7:** Correlation between  $b$  and Drag for the single pimple at  $Re\ 1000000$ ; the black line represents the drag obtained with the flat plate.

The effect of the Area Ratio with the blockage value as a parameter can be studied; to do this, the value of "b" that guaranteed the lowest drag was kept constant, and the other parameters were changed in function of this (eq.4).

$$offset_{pimple} = 0.001 + 1 - \frac{diameter_{pimple}}{2} \quad (4)$$

From the computations, it seems that the area ratio has an influence on the drag produced, as it can be seen in figure 8.

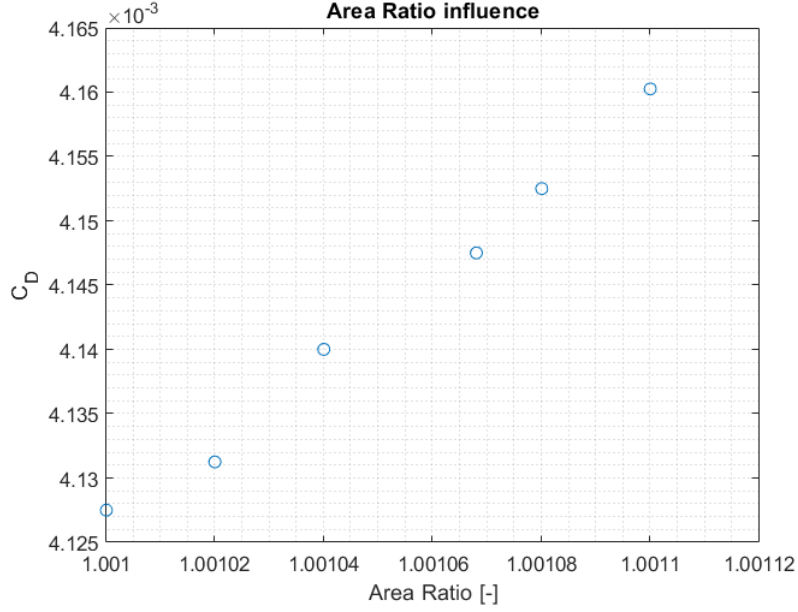


**Figure 8:** *Effect of the area ratio in 6 cases that have the same value of the  $b$  parameter, equal to 0.001 m.*

The Area Ratio is defined as the total length of the flat plate with the pimple divided by the length of the clean flat plate. From those computations it can be found that best pimple's case is achieved with a  $b$  of 0.001m and AR of 1.00026 that guarantees  $C_D = 0.004071$ . When the double pimple configuration will be tested, it may be important to see how extended the recirculation area behind the single pimple is; this may be helpful in finding if it has an influence on the drag. To find this, it was evaluated where the X-shear stress changed its sign from a negative value (inside the recirculation area) to a positive value (outside the recirculation where the reattachment occurs). It was studied the recirculation area in function of the blockage and it comes out that the smallest the area ratio, the lower the length of the recirculation is, as it can be seen in figure 9.

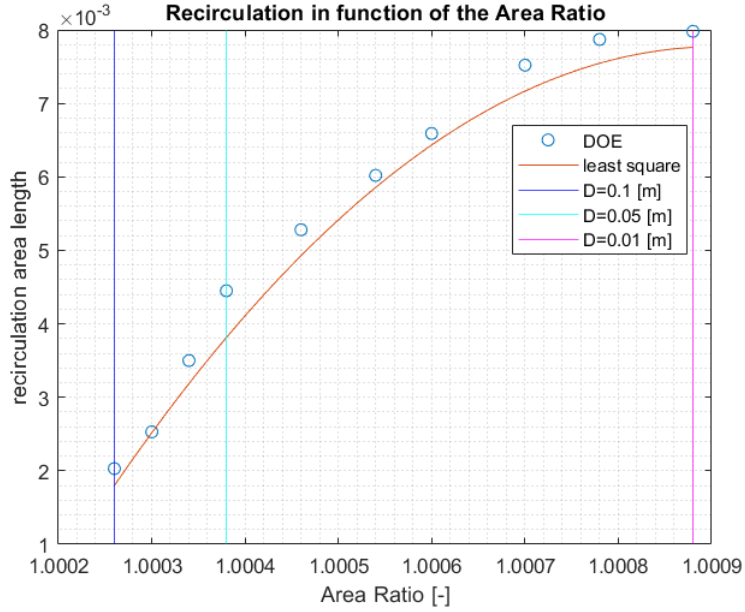


**Figure 9:** *Effect of the Area Ratio on the recirculation area; the vertical lines represents the Area Ratio of three different geometries.*

From what it was obtained so far, the best configurations are the one with the lowest blockage and the smallest Area Ratio; this makes sense because in this way the pimple's case is similar to a flat plate.

#### 4.4.2 "Bigger" dimple

The same DOE was run also with the dimples in the following ranges:

- diameter in the range 0.01 - 0.015m;
- offset in the range 0.002 - 0.004m;.

With the single dimple configuration, the Drag is lower than with the single pimple configuration (in this case the  $C_D = 0.0041$  with diameter of 0.01m and offset of 0.004m); the behaviour is in a certain way similar to the one of the pimple: in fact also in this case the smaller the variation from the flat plate is, the lower the Drag coefficient will be; the results anyway this time are noisier, as it can be seen in figure 11. The RSM for the single dimple can be seen in figure 10.

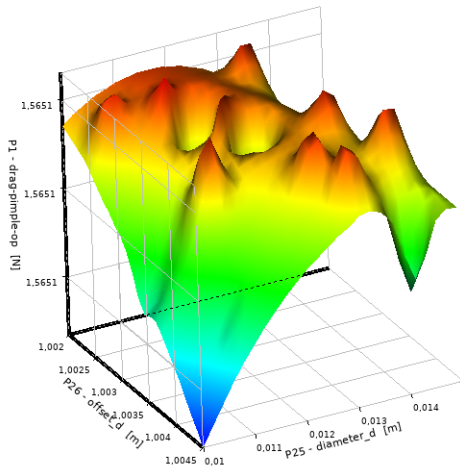


**Figure 10:** RSM of the single dimple configuration at  $Re\ 1000000$  using the Kriging method.

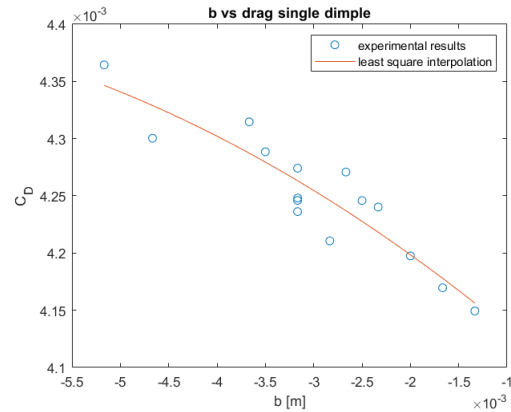


**Figure 11:** Correlation between  $b$  and Drag for the single dimple at  $Re\ 1000000$ .

As for the single pimple, also for the single dimple it was studied how the drag is affected by the shape (or Area Ratio) of the dimple, with the blockage as a parameter. It was obtained a trend that can be seen in figure 12. As for the pimple's case, the smaller the Area Ratio is, the lower the drag becomes.

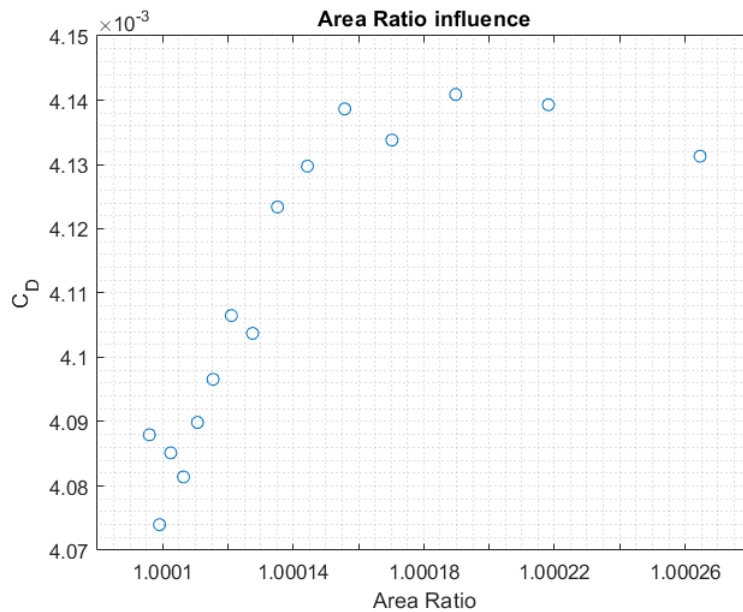


**Figure 12:** Effect of the Area Ratio on the Drag caused by the dimple with  $b$  as a parameter and set to  $0.001m$ .

From an analysis of the results of the Area Ratio it can be seen that it is achieved a  $C_D = 0.004074$ , for the case with the smallest Area Ratio.

### 4.4.3 Double pimple

Double pimple configuration DOE was run with the following constrains:

- the ranges were chosen to have a low blockage to make them generate the lowest drag as possible;
- the minimum spacing was chosen to avoid the pimples to collapse one inside of the other.

To see if also for a double pimple case the best solution was the one with the highest Area Ratio, it was put the diameter as a parameter, and for each case the pimples were free to move in a defined range (Tab.1). The offset was fixed to the one that guaranteed the lowest drag in the single pimple (that means the lowest blockage between the one tested). That choice comes out from a first experiment where the pimples were free to move and the best results were obtained with that value.

diameter [m]	min spacing [m]	max spacing [m]	best $C_D$	best spacing [m]
0.1	0.022	0.3	0.00408	0.036
0.05	0.015	0.3	0.0041	0.047
0.01	0.007	0.3	0.0042	0.03

**Table 1:** Ranges of variations for offset and spacing in function of pimple's diameter.

The Area Ratio for each one is:

1. AR=1.00054;
2. AR=1.00076;
3. AR=1.00174.

As for the other experiments, the lowest Area Ratio guaranteed the lowest drag. If the drag vs. spacing is plotted, it can be found a constant behaviour until a certain spacing, and that value is approximately around 0.2m; in fact for higher spacing than that, the drag seems to start growing. With reference to figure 9 it seems that there's no influence of the recirculation area on the behaviour of the drag in respect to spacing, because that length (at least for the low Area Ratio geometries taken in account) is smaller than the minimum spacing tested.

### 4.4.4 Double dimple

Double dimple DOE was run with the same constrains of the double pimple's one; the shapes of the dimples are the one that gave the best results, which means low blockage and low Area Ratio (diameter of 0.1m and b of 0.001m); the range of variation for the spacing is between 0.023m and 0.2m.

The result of the computations gave a minimum  $C_D = 0.004087$ , that makes the double dimpled surface almost equivalent to the double pimples one.

### 4.4.5 Pimple dimple

In the design of the pimple dimple configuration, it was kept in mind what was found in the previous computations:

- the Area Ratio was kept low;
- the spacing between the geometry was kept low (lower than 0.2m) to avoid the increasing of the drag found before.

It was built the RSM for that case, using the best geometries for the pimple and dimple; those were free to move but the Drag Coefficient wasn't affected by the spacing and remained in the interval 0.0041 and 0.004075.

Also with this geometry, there's no improvement compared to the single pimple case.

#### 4.4.6 Dimple pimple

The same general guidelines used for the pimple dimple geometry were kept also for this case.

As the previous geometry there's no significant dependency of the drag in function of the spacing, and the value stays in the range between 0.004075 and 0.0041.

### 4.5 Best case

The best case between the ones that were tested so far, is the **single pimple** with a small blockage thickness and a large Area Ratio, as it could be expected because that shape is the one that most resembles the flat plate. Anyway, also the double pimple geometry is very similar in terms of drag.

In Tab.2 can be seen the drag (decomposed in total and viscous) for three different shapes of the single pimple configuration (which means with different Area Ratio, while the blockage was kept constant) and for four different Reynolds numbers: from 1 million to 4 million. The values in the table are, respectively, the values of the total drag and of its viscous component.

case	b [m]	AR [-]	1M	1M v.	2M	2M v.	3M	3M v.	4M	4M v.
1	0.001	1.00088	1.696	1.575	6.060	5.546	12.754	11.628	21.617	19.693
2	0.001	1.00026	1.628	1.605	5.756	5.685	12.082	11.945	20.468	20.247
3	0.001	1.00038	1.633	1.595	5.768	5.648	12.106	11.874	20.509	20.137

**Table 2:** Drag Decomposition for four different Reynolds numbers and three different shapes of the single pimple case.

By calculating the  $C_D$  it was found that the simple pimple, with a  $C_D = 0.004071$ , was the best geometry; in fact it is the one that causes the smallest drag increase, between the ones tested.

In the following plots it can be seen the Velocity Magnitude for each shape of the pimple, and for each Reynolds number; they are grouped as it follows: Fig.13, 14, 15 and 16 are relative to case 1, while Fig.17, 18, 19 and 20 are referred to case 2, and finally Fig.21, 22, 23 and 24 are referred to case 3.

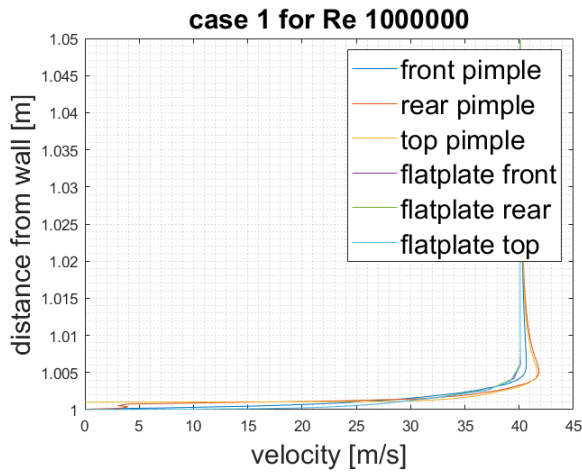


**Figure 13:** Velocity profiles on the leading edge, top and trailing edge of the first case of the table.  $Re=1000000$ .

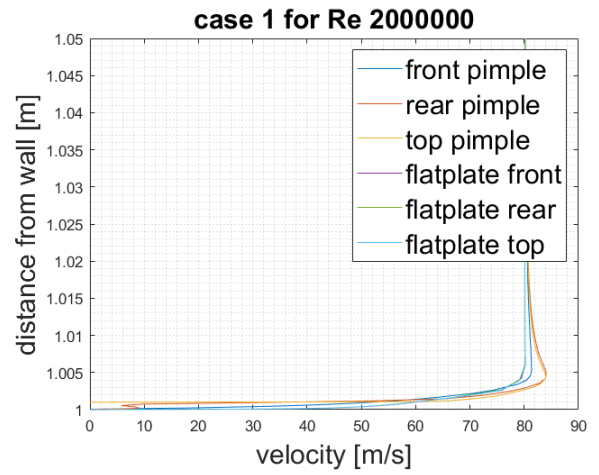


**Figure 14:** Velocity profiles on the leading edge, top and trailing edge of the first case of the table.  $Re=2000000$ .

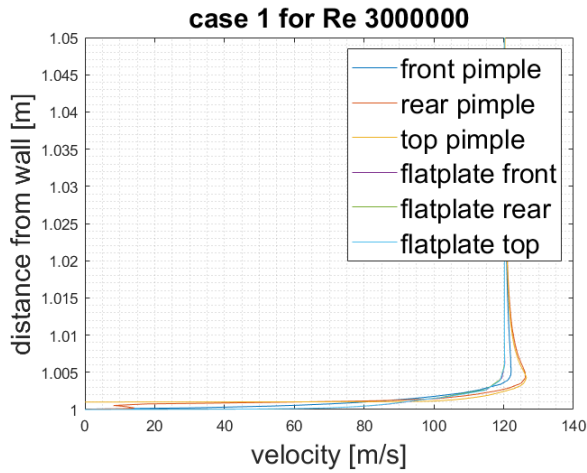


**Figure 15:** Velocity profiles on the leading edge, top and trailing edge of the first case of the table.  $Re=3000000$ .

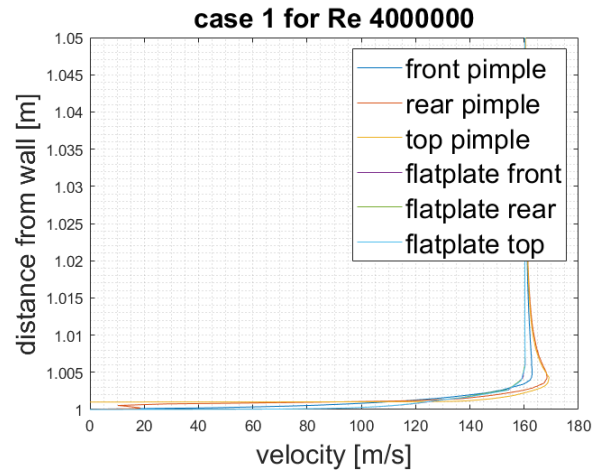


**Figure 16:** Velocity profiles on the leading edge, top and trailing edge of the first case of the table.  $Re=4000000$ .

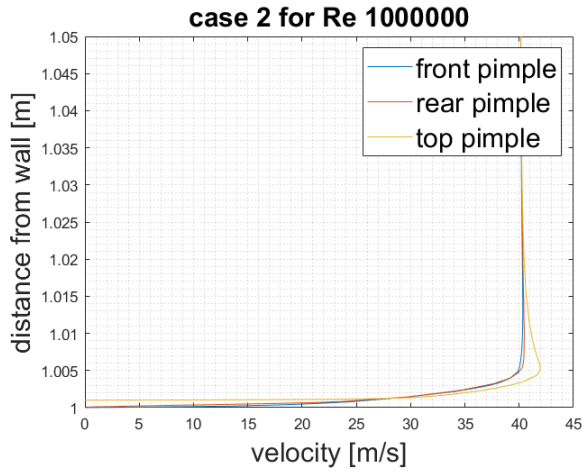


**Figure 17:** Velocity profiles on the leading edge, top and trailing edge of the second case of the table.  $Re=1000000$ .

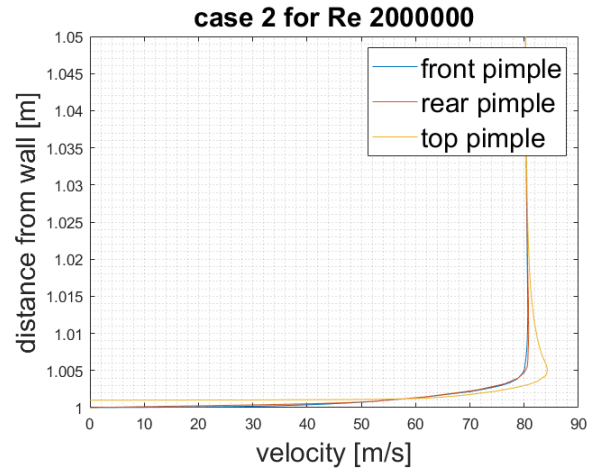


**Figure 18:** Velocity profiles on the leading edge, top and trailing edge of the second case of the table.  $Re=2000000$ .

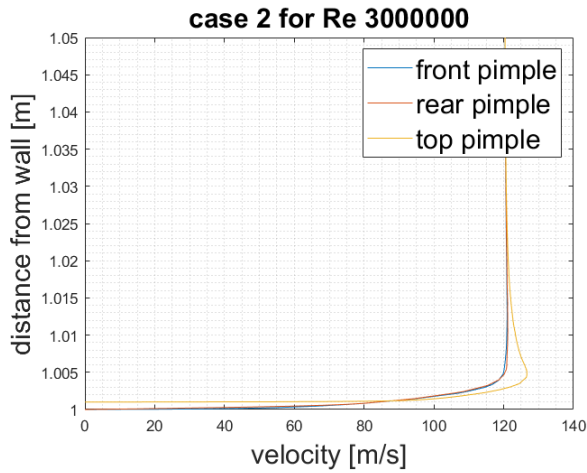


**Figure 19:** Velocity profiles on the leading edge, top and trailing edge of the second case of the table.  $Re=3000000$ .

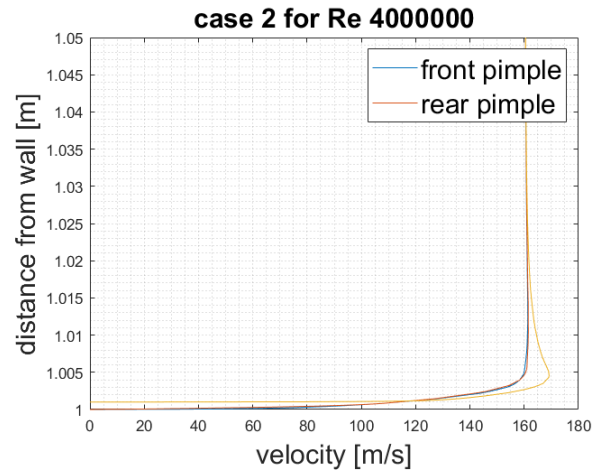


**Figure 20:** Velocity profiles on the leading edge, top and trailing edge of the second case of the table.  $Re=4000000$ .

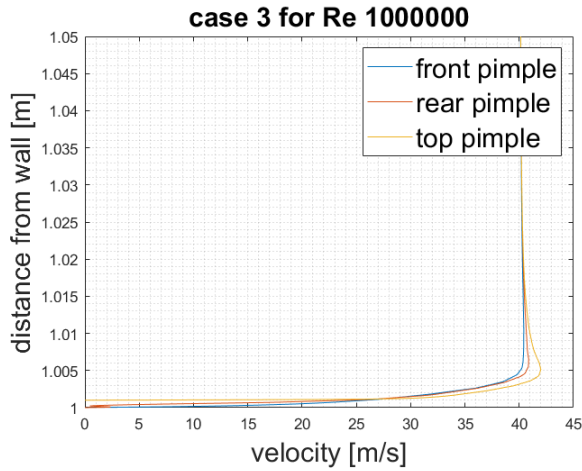


**Figure 21:** Velocity profiles on the leading edge, top and trailing edge of the third case of the table.  $Re=1000000$ .

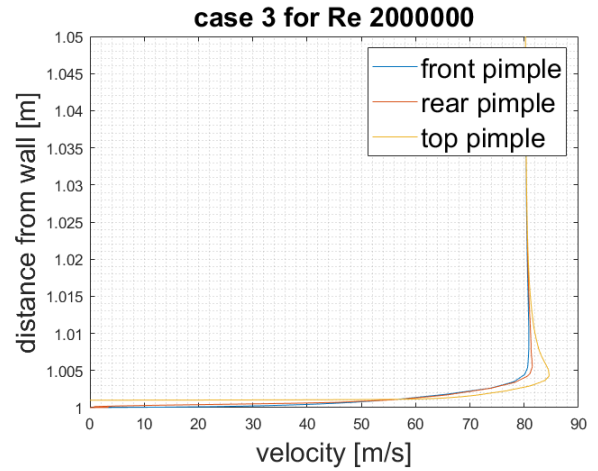


**Figure 22:** Velocity profiles on the leading edge, top and trailing edge of the third case of the table.  $Re=2000000$ .

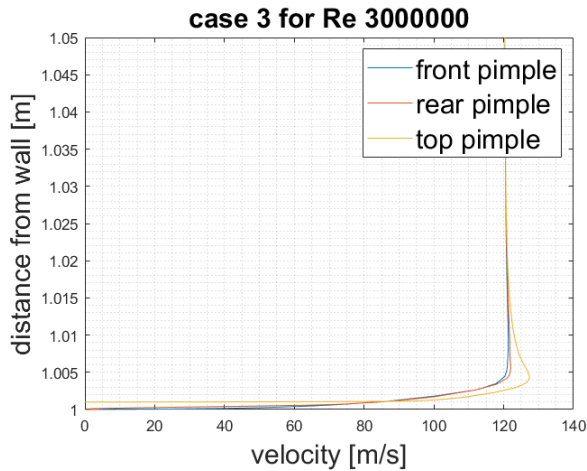


**Figure 23:** Velocity profiles on the leading edge, top and trailing edge of the third case of the table.  $Re=3000000$ .

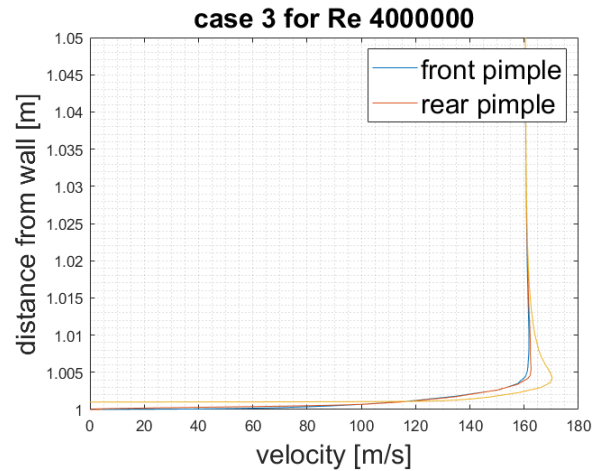


**Figure 24:** Velocity profiles on the leading edge, top and trailing edge of the third case of the table.  $Re=4000000$ .

In the plots it can be seen (only in the lines referend to the Trailing Edge) a small region, close to 0, where the profile is sharp and that represents a recirculation area: the "flattest" the pimple is, the smallest that region is and the smallest the drag. That drag reduction is constant for every Reynolds number but, if decomposed, it can be seen that the viscous part of the drag has the opposite behaviour; in fact it is smaller with the highest Area Ratios and then tends to increase.

For the best pimple configuration, it was run a simulation with the transition SST model to find out where it was the optimal position of the pimple in respect to the point where transition occurs; the pimple was moved in three different positions respectively before, on and after the coordinate where transition occurs (that corresponds to 1m, 1.2m and 1.4m from the inlet). Results of those simulations can be found in the plots of figures 25 and 26.

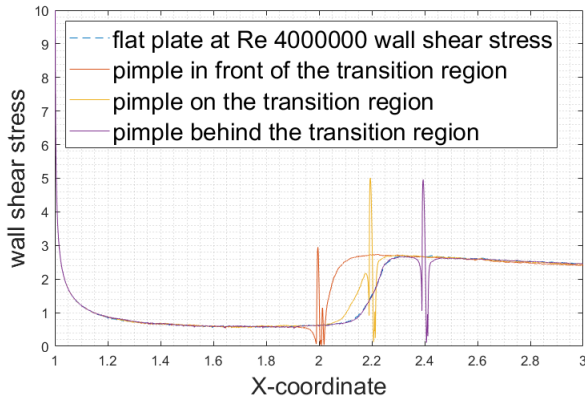


**Figure 25:** Wall shear stress for the flat plate and for the pimple case, in three different positions at  $Re\ 1000000$ .

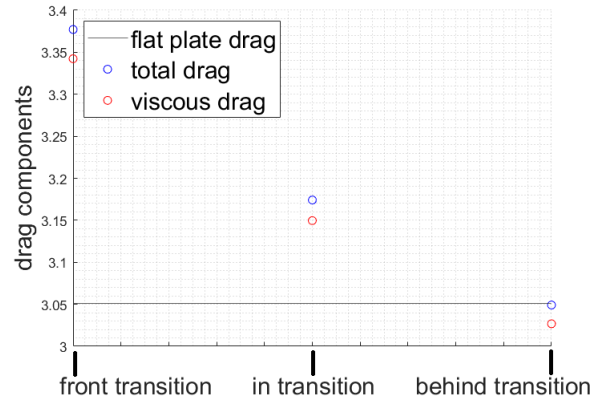


**Figure 26:** Drag decomposition for the three configurations of the pimple at  $Re\ 1000000$ .

For the case of pimple behind the transition point, it has been plotted the  $y^+$  vs  $u^+$ ; in figure 27 can be found the comparison of the non-dimensional velocity plot of the flat plate with pimple and the simple flat plate; from the plot it comes out that the behaviour is the same.

In figures 29 and ?? the non-dimensional velocities evaluated on the leading edge and on the trailing edge of the pimple were plotted.

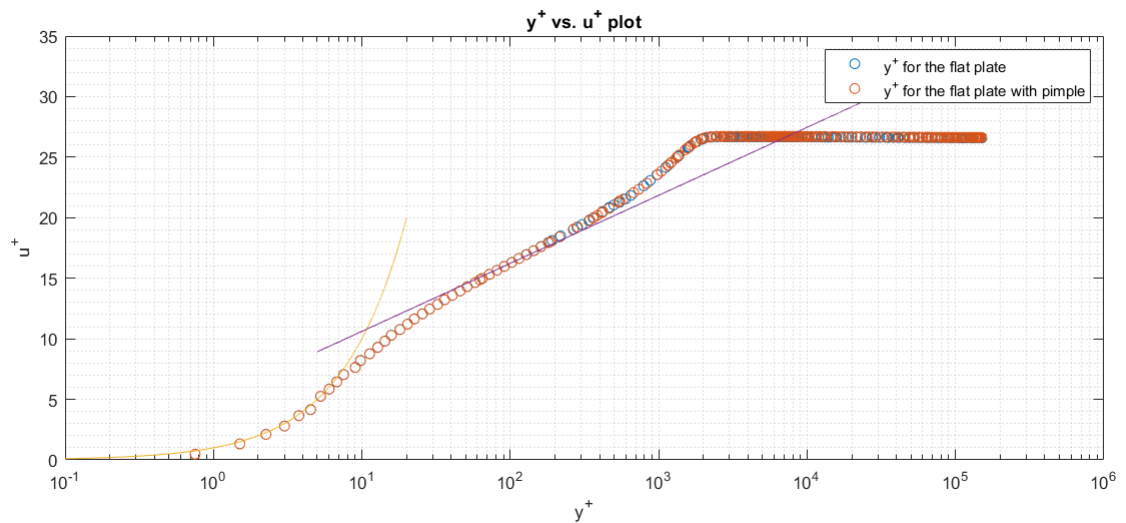


**Figure 27:**  $y^+$  vs  $u^+$  for the case of the flat plate with pimple and the clean one calculated at the same coordinate.

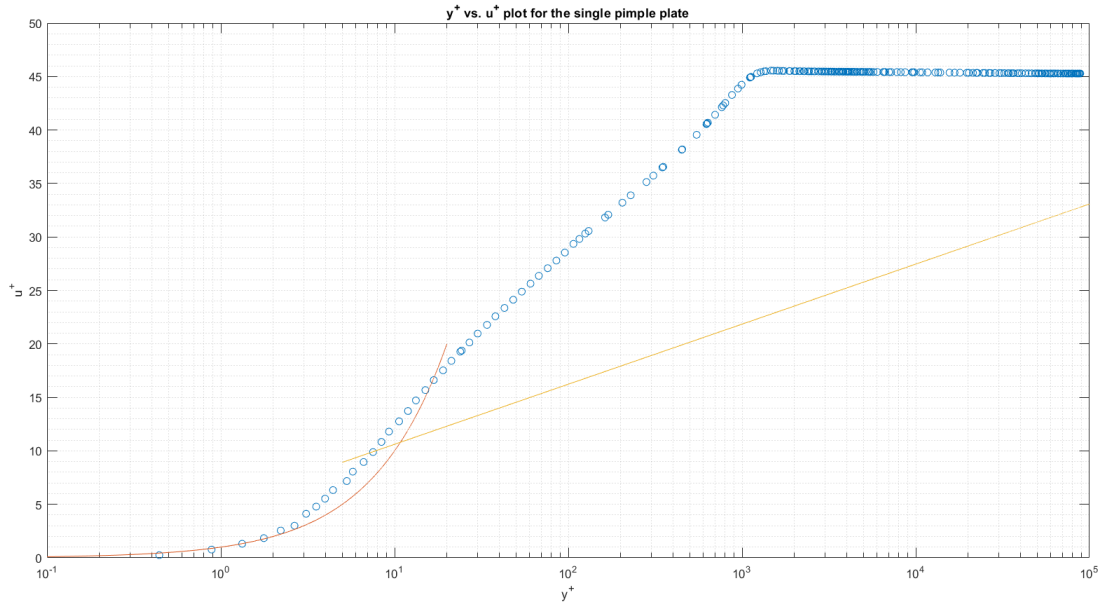


**Figure 28:**  $y^+$  vs  $u^+$  plot in front of the pimple.

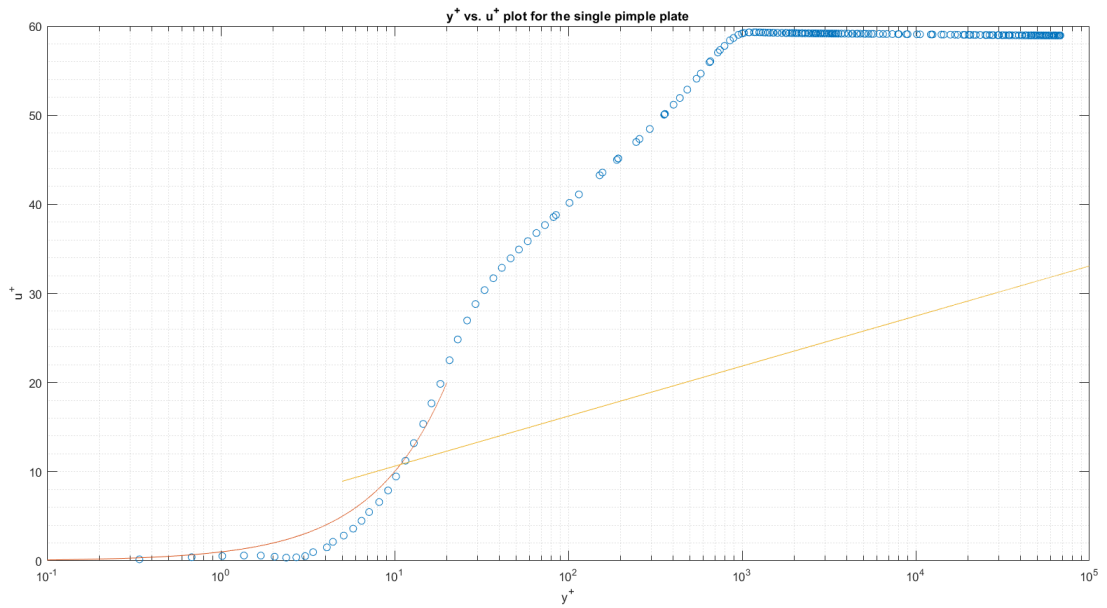


**Figure 29:**  $y^+$  vs  $u^+$  plot in front of the pimple.

From those plots, it comes out that right before and after the pimple, the behaviour of the non-dimensional velocities are above the log-law and this means that the velocities keep following the viscous sublayer behaviour for a short section; here the flow is laminar and not turbulent and for this reason the viscous drag will be lower than on the rest of the plate, where there's turbulent flow. This can also be seen directly in the wall shear stress plot in fig.30.

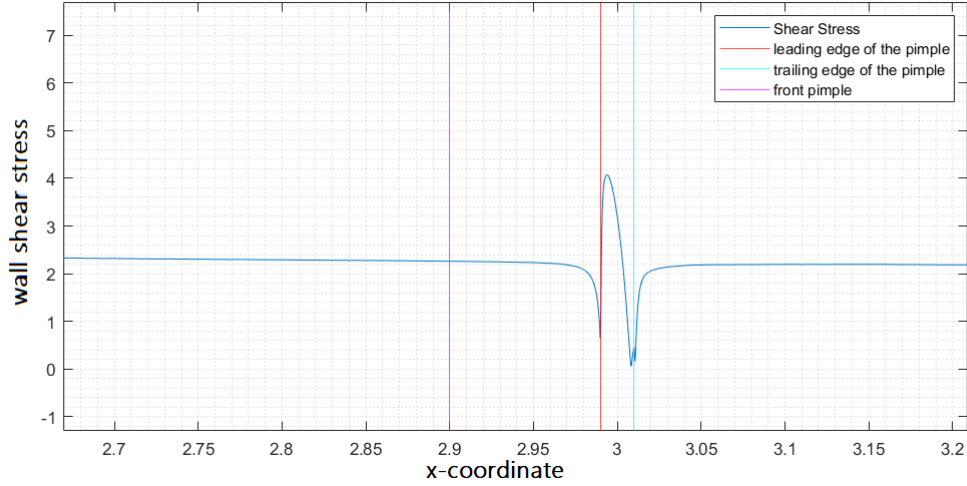


**Figure 30:** Wall shear stress plot with reference lines for the pimple leading edge and trailing edge and the reference plot line.

Behind the pimple, there's a small recirculation region, which implies a lower velocity at the wall, with a resulting lower viscous drag. Instead, on the leading edge, the pimple causes a reduction of the velocity of the flow caused by stagnation, that makes the boundary layer thickness increases with the pressure. The pressure at the wall can be seen in figure 31.

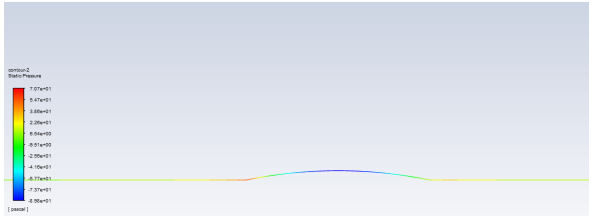


**Figure 31:** Static pressure at the wall close to the pimple

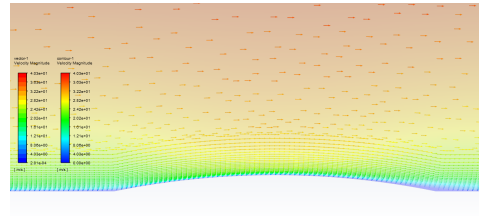


**Figure 32:** Contours and vectors of velocity magnitude around the pimple.

## 4.6 Conclusions

From the 2D calculations, it was obtained that the best geometrical configuration (to have the smallest drag in respect to the flat plate) is the single pimple configuration. The double pimple configuration, anyway, is close to the best one and, in the 3D case, it could be interesting to study the interactions between pimples and their wakes, to find if there's a location of those devices, that varies the drag. A summary of what it was found can be seen in Tab. 3.

case	Drag force normalized on the flat plate	Percentual variation in respect to the flat plate	$C_D$
high AR pimple	1.083	8.3%	0.0042
high AR dimple	1.056	5.6%	0.0041
low AR pimple	1.0435	4.4%	0.004071
low AR dimple	1.044	4.5%	0.004074
low AR double pimple	1.046	4.6%	0.00408
low AR double dimple	1.048	4.8%	0.004087
low AR pimple dimple	1.044	4.5%	0.004075
low AR dimple pimple	1.044	4.5%	0.004075

**Table 3:** *Resume of the results found.*

## 4.7 Optimization

For the optimization of pimple's shape, it was chosen the adjoint method; it was first run a direct case with only a convergence criteria for the continuity to  $10^{-6}$ , that was reached in around 180 iterations. The setup for the adjoint is the following:

- it was chosen a force observable and it was applied to the wall, and the objective orientation was set to minimize;
- to use the adjoint properly it was made reference to [4]; the solution method chosen for the adjoint solver was the Green-Gauss Cell Based with Default options for Pressure and Momentum; that choice was made to avoid the solver to become unstable;
- the Adjoint Residual convergence criteria monitors were set to  $10^{-6}$  for continuity and adjoint velocity, while was left the default value for Adjoint local flow rate;
- for the Design it was chosen a box of morphing that included the whole pimple.

For first iteration, it was chosen a desired reduction of drag of -0.5% and the shape obtained by the morphing of the pimple can be seen in fig.33. Drag coefficient before the morphing was  $C_D = 0.00389$ , while after the first iteration became  $C_D = 0.00388$ ; that corresponds to a lower reduction than the expected one: -0.3% against the expected -0.5%.

The morphing caused by the adjoint was predictable; in fact, to reduce the drag, it tries to flatten the pimple to make it closer to a flat plate.

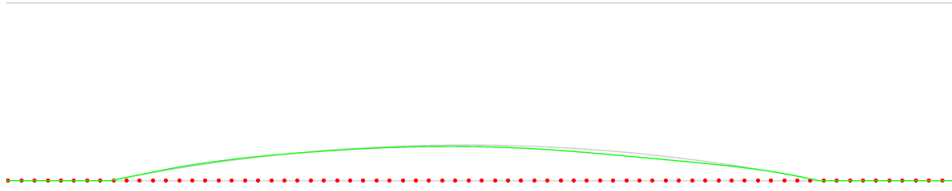


**Figure 33:** *Shape morphing obtained with the adjoint method.*

Other two iterations were run and each one with a desired percentage reduction of the drag of -1%; from those, it was obtained relatively:  $C_D = 0.00387$  and  $C_D = 0.00385$  that correspond to a reduction of -0.3% and -0.5%. From the first of those two iterations, is obtained the shape in fig.34 and, from the second, a similar shape that differs mainly in the rear of the pimple, where the focus was made (figure 35).

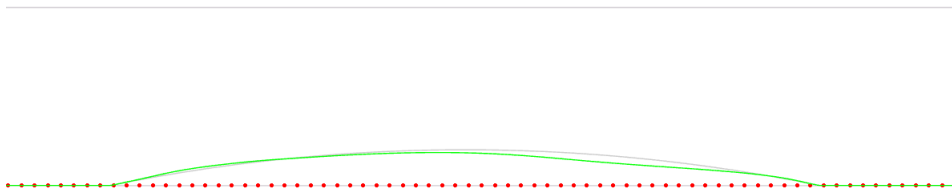


**Figure 34:** *Shape morphing of pimple's geometry obtained with the first of the two iteration with a drag objective reduction of -1%.*



**Figure 35:** *Shape morphing of pimple's geometry obtained with the second of the two iteration with a drag objective reduction of -1%.*

Those results show that the best solution that will be reached with further adjoint's iterations, will be to totally flatten the pimple to recreate a simple flat plate.

## 5 Part 2: 3D flat plate: single device

This computation was made to understand what are the main characteristics of a flux near a single pimple/dimple whose free parameters are those reported in the following drawing: offset and diameter. These two parameters correspond to the way this geometry is generated: in both cases a sphere is subtracted or added by a Boolean operation to the main rectangular extrusion to make the pimple or the dimple. This was the easiest way to generate both geometries in the least number of steps.

The operating conditions are chosen to have a  $Re_l = \frac{\rho v l}{\mu} = 10^6$  on the pimple, where "l" is the distance between the center of the pimple/dimple and the leading edge of the flat plate. For this reason and taking into account that we are in incompressible, Newtonian, isothermal regime, we can get this  $Re_l$  by changing  $l$ ,  $\mu$ ,  $v$  at the same time. The values taken in this case are:

- $\rho = 1.225 \text{ kg/m}^3$
- $\mu = 3.43 \cdot 10^{-6} \text{ kg/ms}$
- $v = 40 \text{ m/s}$
- $l = 0.07 \text{ m}$

### 5.1 Geometry and mesh

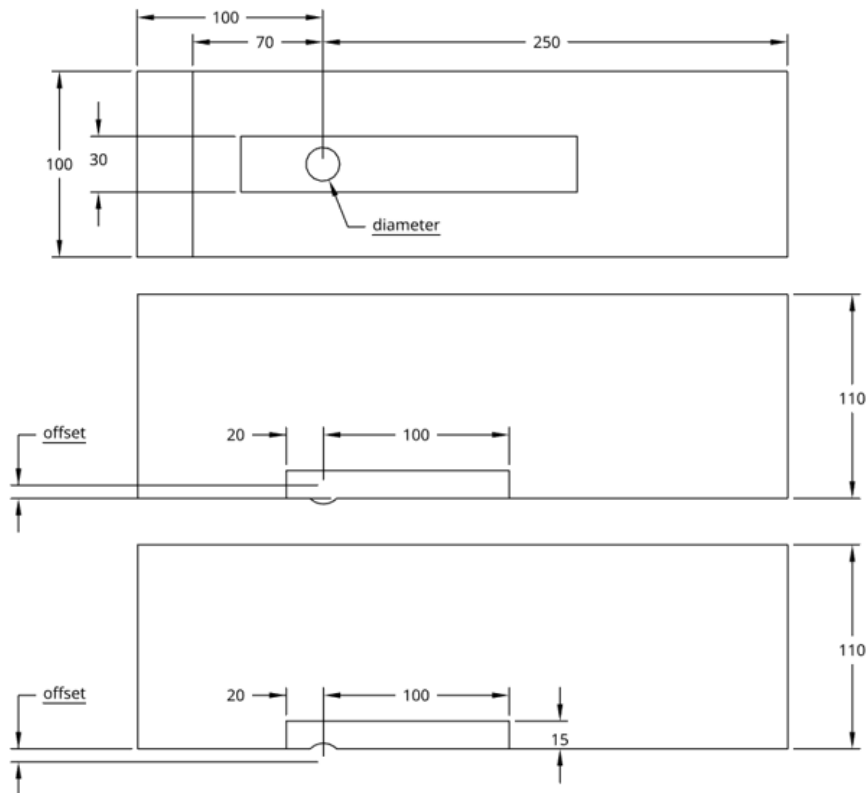


**Figure 36:** 3D fluid domain in case of pimple and dimple, dimensions are in [mm], geometrical parameters are underlined

The fluid domain was chosen after some iterations to have at the same time a good approximation of the external aerodynamics conditions (i.e. no pressure gradients induced by the interaction with the lateral walls), a reasonable number of cells (no more than 512 000, in our case about 300 000 using "make-polyhedra" in Fluent) and  $R_L = l_0/l_{cell} \approx 3$  in the zone near the pimples/dimples for most of computations (this is the lowest acceptable value of this parameter for a RANS: a  $R_L$  of about 5 should be more indicated, but for the moment we have to accept this limit as it is only a preliminary computation). The height of the fluid domain is 20 times the maximum blockage height considered in this case, while laterally there are more relaxed limits. Downstream to the pimple/dimple there is a refined body of influence to capture the horseshoe vortices generated by the pimple or the "cyclone" generated by the dimple. Of course, it would have been better to lengthen the body of influence until the end of the domain, but this would have required too many cells, so some numerical diffusion was accepted as a good compromise.

The mesh in this case was obtained with Ansys mesher, using the following parameters:

- mesh max size: 25mm
- body of influence: element size 2.8mm
- face sizing on the bottom sides: 2,8mm, curvature max angle 5 °
- inflation layers: first layer height 0.005mm, growth rate 1.16, 31 layers

and then the mesh was converted to polyhedral in Fluent. This passage allows a more rapid and less oscillatory convergence, certainly desirable to reduce the number of operations needed to get a correct estimate of the output parameters. The mesh is set for a wall resolving approach and, to get a uniform value of wall  $y+$ , the inflation layer was applied also in the "entrance" region, that has a "symmetry" boundary condition, so it wouldn't need a wall treatment.

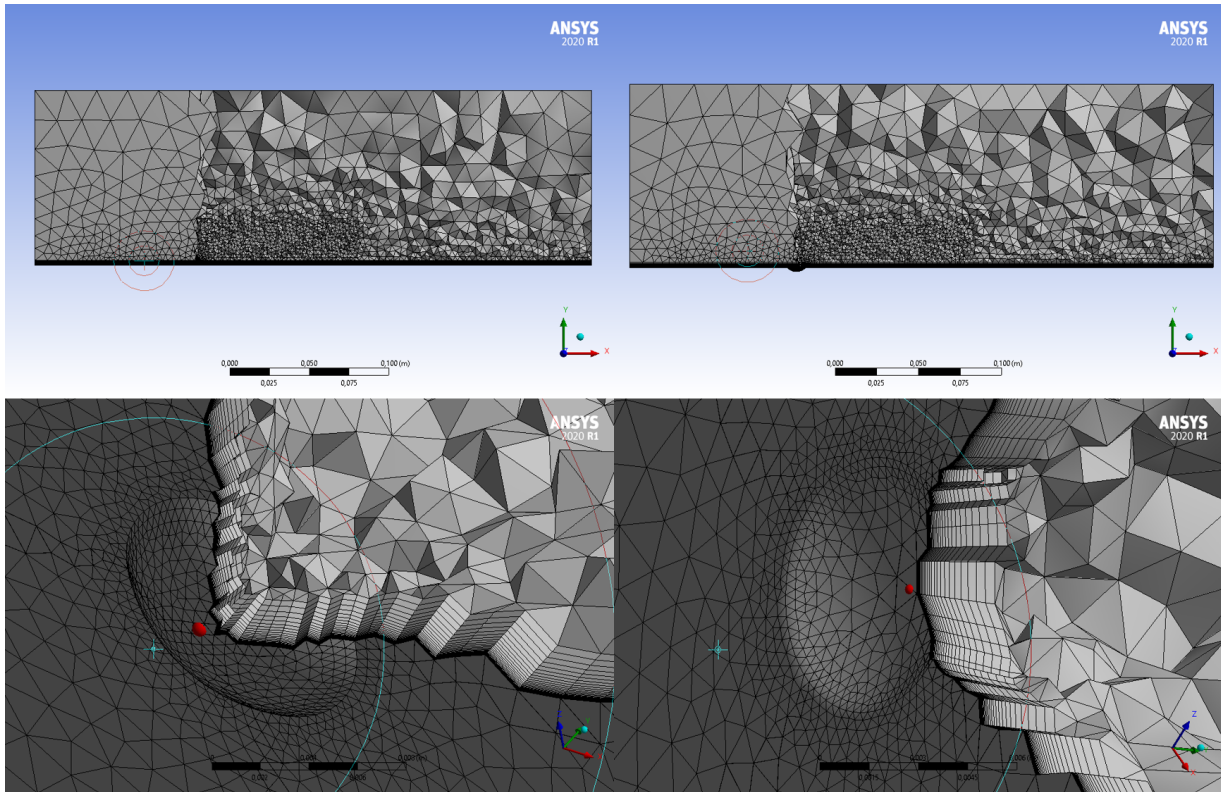


**Figure 37:** sections of the meshes for single pimple and dimple before the conversion to polyhedral in Fluent. The skewness remains always under 0.85 and the orthogonal quality is always higher than 0.14

## 5.2 Setup

The setup was made considering that, to have a stable behaviour, the top and lateral boundaries of the domain couldn't be set as "pressure-outlets" but had to be set as symmetry walls: this allowed the program not to compute reverse flows which would have made the solution unstable and let the flow go without the no-slip condition, but could have had an influence on pressure distribution, which was verified to be negligible, above all for a small pimple/dimple. The boundary conditions are:

- velocity inlet: velocity magnitude: 40 m/s, directed along x-axis, Turbulence Intensity 1%, viscosity ratio 2 (external aerodynamics conditions)
- pressure outlet: gauge pressure zero (operating pressure is 101325 Pa)
- plate and device: no-slip wall, default roughness
- left, right, top, entrance: symmetry

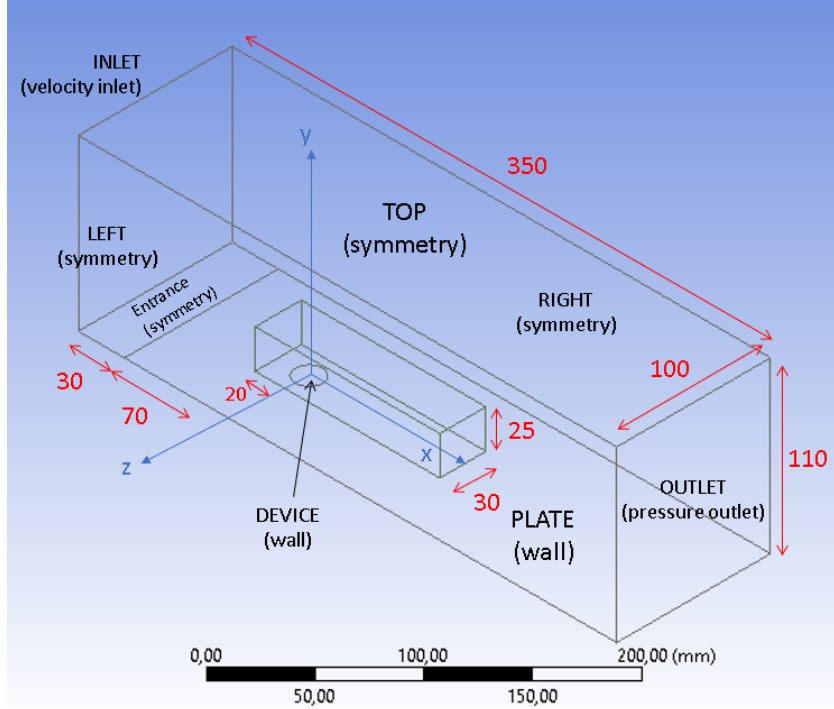


**Figure 38:** zone names and boundary conditions, dimensions are in [mm]. the surface of the flat plate is  $S = 0.032m^2$

The turbulence model is the *SST*  $k - \omega$ , which is able to go low-Re and is suitable also for a wide range of problems: in this case the model was corrected using the production limiters (the pimple/dimple is a bluff body, above all in case of big ones) and curvature correction to cope with the horseshoe vortex and the dimple's "cyclone". The setting coefficients were kept as default, as there was no possibility to go for a calibration of these parameters: no similar studies are, in fact, available in literature.

The fluid (air) properties were kept as default except for the dynamic viscosity, whose value was changed to  $\mu = 3.43 \cdot 10^{-6} \text{ mg/ms}$  as previously described.

The pressure-velocity coupling technique is the COUPLED, which allows a faster convergence but has a higher cost per iteration. The pseudo-transient formulation was switched on and left with the default parameters and, to cope with warped faces in the polyhedral mesh, the corresponding correction was enabled, accepting an increased cost per iteration. The under-relaxation factors were left as default or decreased a little in case of oscillatory behaviour. In that case, resulting force reports were averaged over the last 20 iterations. Convergence was generally reached before 160 iterations.

Reports of  $y+$  (average, max, min), mass-flow-rate imbalance between inlet and outlet, drag on the plate and the device and the integral of x-wall shear stress were created. Pressure drag on the device (which is the only component with non-zero projected area in the streamwise direction x) is computed as

$$D_{press} = \sum_i p_i A_{x,i} = D_{tot} - D_{visc} \quad (5)$$

where

$$D_{visc} = \int_S \int \tau_x dA \approx \sum_i \tau_{x,i} A_i \quad (6)$$

The solution was initialised in the standard way, computing from inlet: most of the domain is, in fact, at the inlet velocity, so this should be a good initial guess. However, initializing with full-multi-grid or with a converged solution on a flat-plate doesn't result in big differences on the convergence rate.

The solution shows a rapid transitory that lasts until about 70 iterations, then becomes stable/oscillating. Residuals show a rapid descent at first and then stabilize or decrease less rapidly. These behaviours are due to the intrinsic unsteadiness of most of cases: if the pimple/dimple is bigger, the vortex shedding is strong enough to perturbate the solution (an unsteady simulation would be required to capture better this behaviour) while for small devices the RANS simulation is much closer to reality, as vortex shedding is negligible.

### 5.3 Results

The single-device geometry was studied with a device-diameter between 15 and 21.5mm and an offset between 5 and 7mm: these limitations were chosen in such a way that the device never becomes too big for the chosen domain nor its shape becomes too flat or abnormal (the slope of the device LE should always be of the same sign). Then, to confirm the trends, some refinement points were added.

Some quantitative and qualitative post-processing was made on these simulations to identify the most important flow structures: first a qualitative analysis of Q criterion iso-surfaces in case of big pimples/dimples was useful to identify the coherent structures and understand the working principles of these devices. For this purpose, an iso-surface of Q-criterion was created, where

$$Q = \frac{1}{2} (tr(\nabla \mathbf{u})^2 - tr(\nabla \mathbf{u}^2)) \quad (7)$$

(where  $Q > 0$  points out the presence of a vortex). This iso-surface was calibrated to show the main vortices without losing minor-but-important structures. Over this surface a velocity vector plot was made to show the direction of the recirculating flows. A x-wall shear stress plot was then created in the same "scene" to show whether there are or not correlations between the viscous drag and the main vortices.

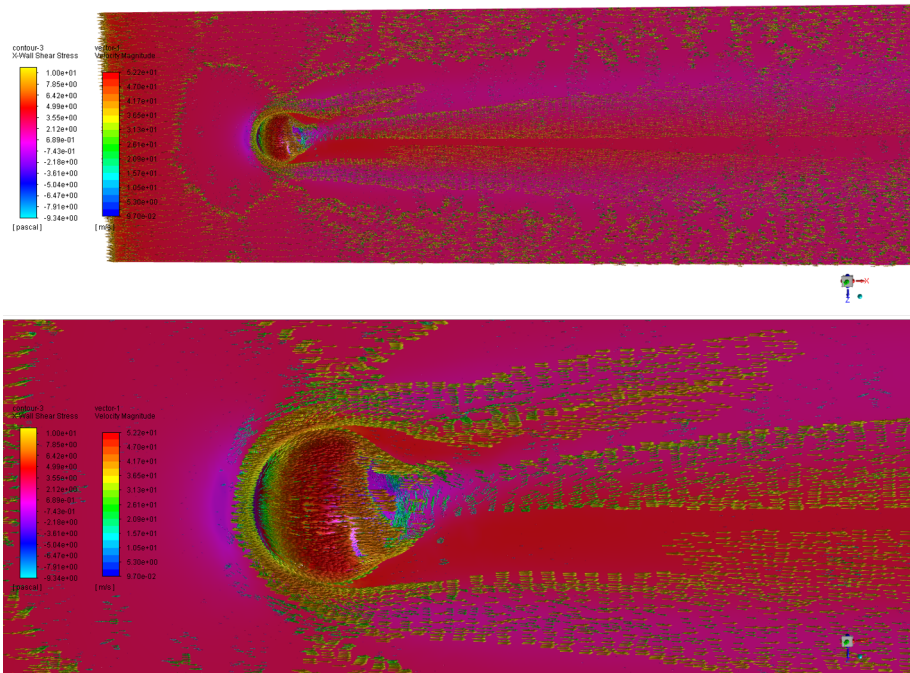


**Figure 39:** *single Pimple: vector plot on Q-criterion iso-surface and x-wall shear stress contour on the plate, general view and zoom on the recirculating zone*

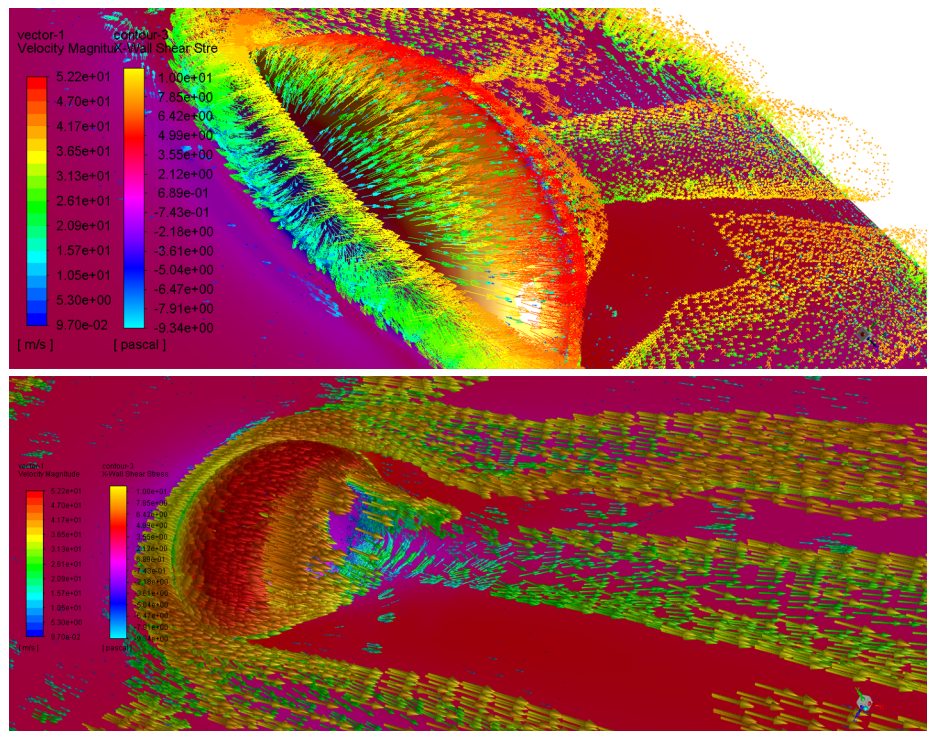


**Figure 40:** *single Pimple: vector plot on Q-criterion iso-surface and x-wall shear stress contour on the plate, detail of the horseshoe vortex and the recirculating zone*

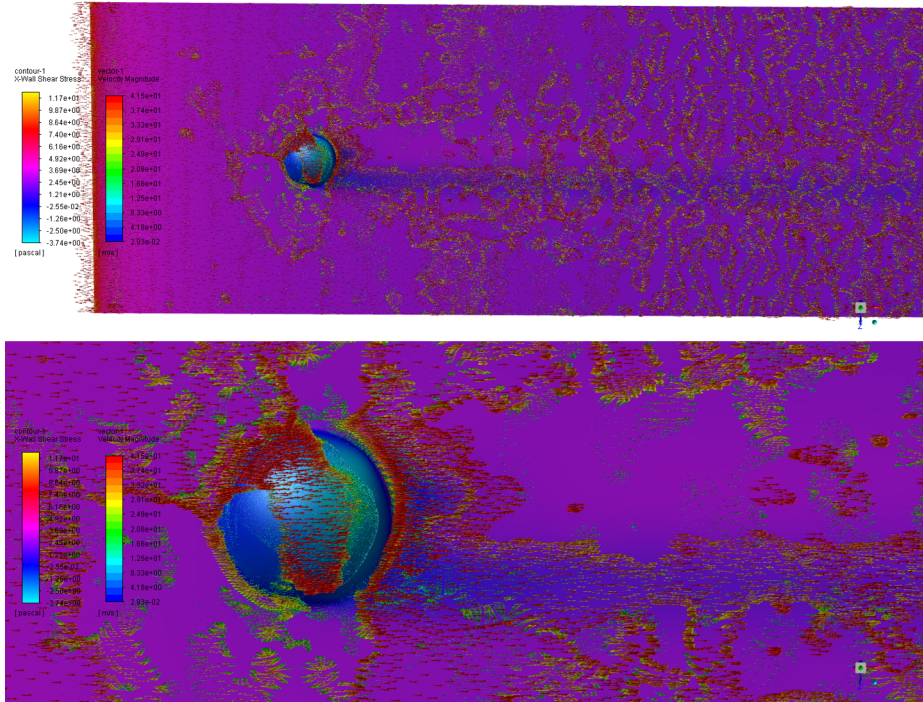


**Figure 41:** *single Dimple: vector plot on Q-criterion iso-surface and x-wall shear stress contour on the plate, general view and zoom on the recirculating zone*

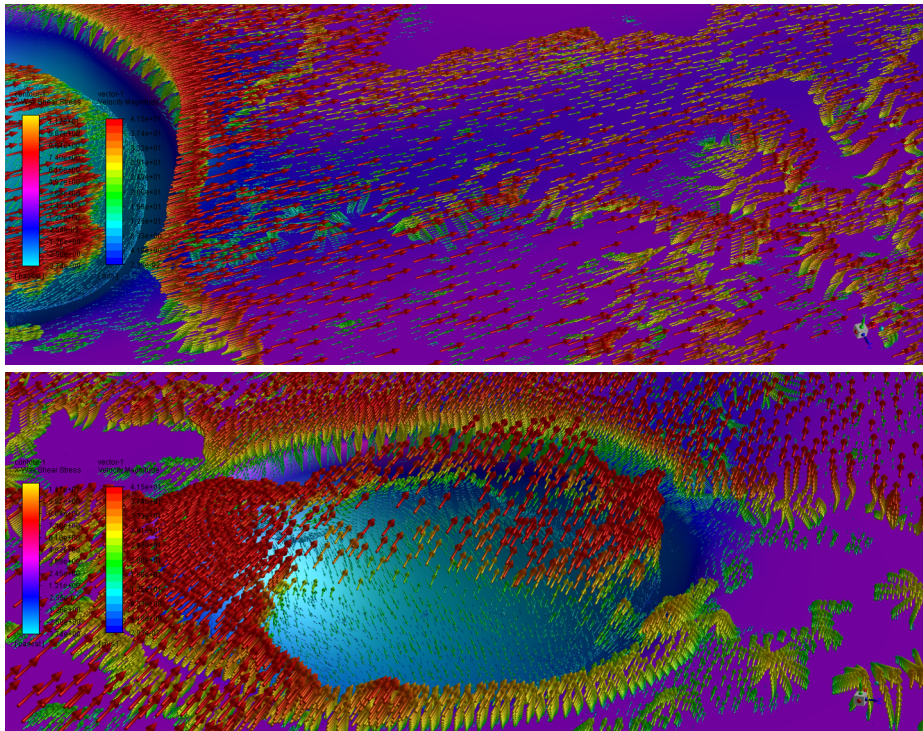


**Figure 42:** *single Dimple: vector plot on Q-criterion iso-surface and x-wall shear stress contour on the plate, detail of the vortex structure: the flow enters the dimple, rotates about the z-axis and, at the same time, the y-axis, generating the cyclone. The cyclone then exits the dimple asymmetrically. This last stage may happen on both sides of the dimple and is very unsteady*

From the previous plots we can say that:

- the pimple, even if shows a region of detached flow, has more stable vortex structures than the dimple, as they become elongated in the streamwise direction nearly immediately. The horseshoe vortex, in particular, shows a strong-vorticity zone in front of the pimple and then the vortex starts diffusing in the wake. Another vortex structure seems to be released from the detached zone. It is not clear if this structure has or not two branches (it should have, according to Kelvin circulation theorem: in the streak some kind of secondary vortex structure seem to appear and its circulation should be conserved)
- the vortices induced by the pimple divide the x-wall shear stress contours in a zone where the stress is higher than that on the flat plate (red) and a zone where it is much lower, nearly negative (fuchsia). The stress is higher where the vortex pushes air towards the wall (flattening the BL) and lower where the vortex pulls air up (heightening the BL without causing separation. The pressure distribution on the pimple, however, causes always a pressure drag and never a thrust, obviously)
- the structure induced by the dimple shows a more unsteady behaviour, as described in [5] and rotates also about the vertical axis, generating a streak that can change lateral position. In this case it is harder to identify the coherent structures: it seems that the structures affect a very limited portion of the domain, on the contrary of the Pimple. Again, the x-wall shear stress in the streak seems only to diminish, without alternating zones of increase and decrease, like in the Pimple case. The viscous drag in the Dimple cavity can be either positive or negative: the bigger the dimple, the more negative the viscous drag. This can be easily explained considering that, for very flat dimples, detachment is much reduced and the cyclone is nonexistent.

To get a quantification of the amount of viscous drag generated by these devices, a plot of friction coefficient of x-wall shear stress along the plate centerline was generated:

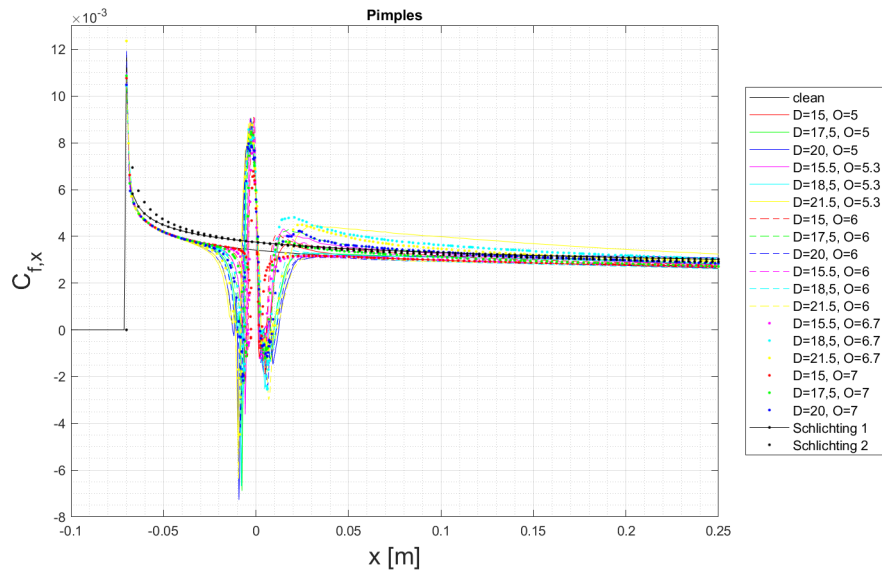


**Figure 43:** *Single pimple:  $x$  wall shear stress friction coefficient vs streamwise coordinate  $x$ . "o" is the offset parameter, "D" is the diameter of the pimple*

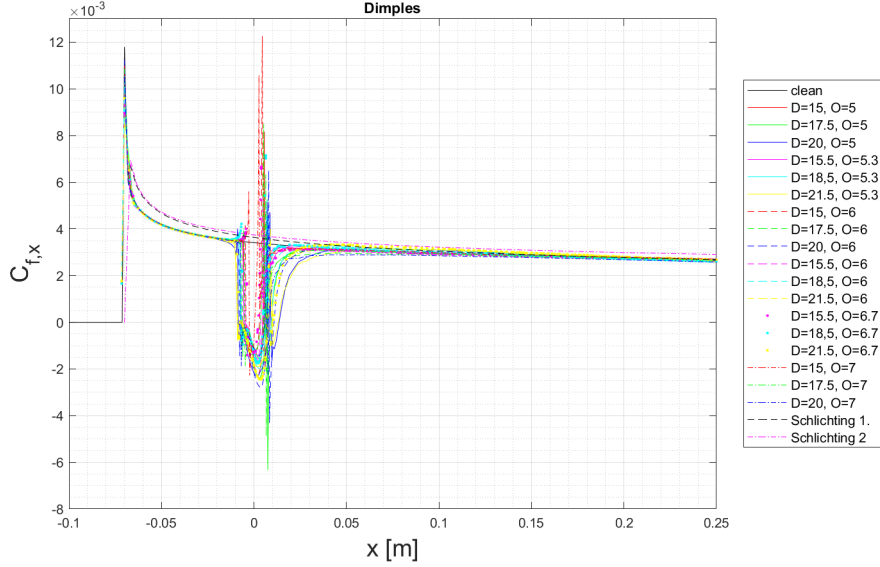


**Figure 44:** *Single dimple:  $x$  wall shear stress friction coefficient vs streamwise coordinate  $x$ . "o" is the offset parameter, "D" is the diameter of the dimple*

where

$$C_f = \frac{\tau_x}{0.5\rho v^2} \quad \tau_x = \mu \frac{\partial u}{\partial y} \quad (8)$$

These plots do not aim at describing completely the generation of viscous drag on the dimpled/pimpled plate, but can be used as a measure of how distant -on the centerline- the effect of a pimple/dimple can be detected and might show some correlation with drag production. For example, a main difference between pimples and dimples is that dimples induce less sharp changes in  $C_{f,x}$  than pimples: this can be explained considering that dimples make a sharp diffusion at their leading edge, forcing detachment, then the flux that does not take part into the cyclone (but runs over it) bumps against the final part of the dimple, causing the second peak of  $C_{f,x}$ .

Another difference is that the pimple causes a variation in the slope of the  $C_{f,x}$  curve: this happens mainly in the zone immediately downstream the pimple, but also a little bit after that. Instead, the dimple shows curves that are much more attached to that of the base flat-plate in the downstream region. This analysis is also coherent with the previous one, done qualitatively on the Q-criterion iso-surfaces. These curves were compared with two correlations by Schlichting for fully turbulent flat-plate, available in literature [6]. The numerical computation underestimates a little bit the friction coefficient at the leading edge of the plate, but then the behaviour is correctly captured downstream.

A similar feature the two plots show is that, even if referred to different sizes of the device, they do not show very sharp changes in the overall behaviour, this suggests that there are no sharp changes in the viscous structures that govern the problem.

To be precise, a comparison between the drag at the centerline and in the zone where the device shows a reduction in  $\tau_x$  may be useful. This comparison is made for simplicity for just one of the previous cases, which corresponds to the worst examined case in terms of drag:

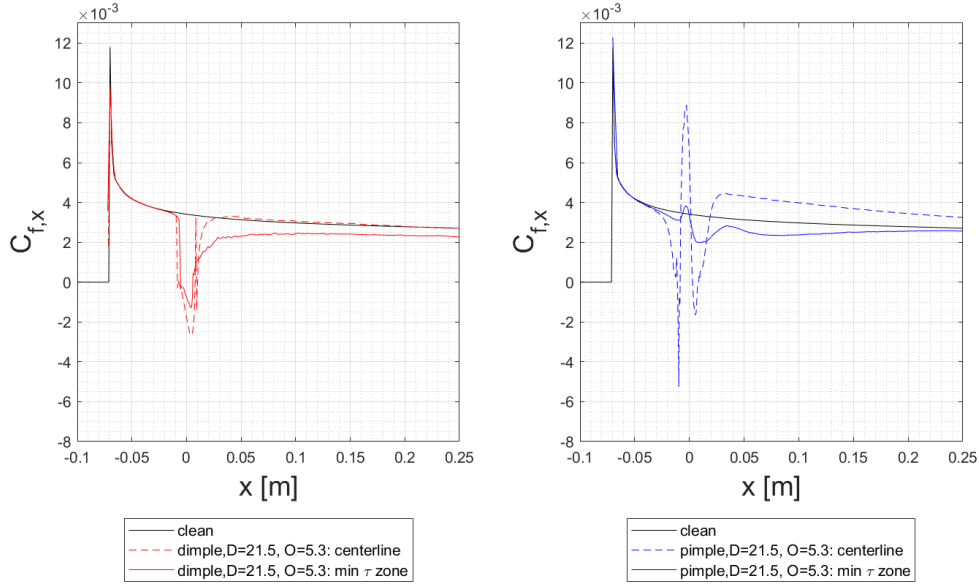


**Figure 45:**  $x$  wall shear stress friction coefficient vs streamwise coordinate  $x$ . "o" is the offset parameter, "D" is the diameter of the pimple/dimple

In the zone where the vortices produce a  $\tau_x$  reduction the  $x$ -wall shear stress shows also a variation in slope, becoming lower than the correspondent flat plate  $\tau_x$ . The Pimple shows zones where  $\tau_x$  is increased and zones where it is decreased, while the dimple shows only a decrease in  $\tau_x$ . One would say that taking into account this result, a dimple is always more efficient than a pimple, but it wouldn't be correct, as we have not discussed pressure drag so far.

At this point, we can say that:

- the zone of viscous-drag reduction provoked by a dimple is only one while a pimple creates alternating zones of viscous-drag reduction and addition. In both cases those zones are elongated in the streamwise direction
- the vortex exiting from the dimple can show a lateral movement in time, while that provoked by a pimple is more steady.
- the zone of viscous-drag reduction provoked by a dimple is generally thinner than those provoked by a pimple
- to optimize viscous drag reduction, a correct juxtaposition of the devices should take into account both longitudinal distance between the devices (as there is a variation in  $\tau_x(x)$  slope) and lateral distance (as there are zones of alternating drag reduction and addition or, however, lateral variations in  $\tau_x$ )

## 5.4 Optimization

So far, we have not discussed pressure drag. It is natural to think that the bigger the projected area in the direction of the flux, the bigger the pressure drag. This relation is qualitatively correct, but it is not trivial to quantify "how big" the device is: till now,

two parameters have governed the geometry: the "offset" and the diameter of the device; from these parameters, other parameters can be generated and maybe one of these could describe the geometry better than the others, making the 3D curve of drag or some drag component collapse on a single 2D curve. This would drop one useless parameter. In the same way, we might say that there could be a relation between some characteristic lengths of the flux (end of the recirculating zone, distance between end of the device and end of the recirculating zone...) and drag. For this reason, a cumulative plot where quantities of interest are plotted versus possible parameters is presented in fig. 46 and 47, below. In those figures it is easy to see that there seems to be a linear trend in the first two charts, but with a certain amount of dispersion, while the drag (or pressure drag) vs  $Re_{h-block}$  shows a very clear trend, that is close to a parabola. Other parameters are not as able as the blockage height to pack the data in this way, so the blockage height seems to be the governing parameter of this problem.

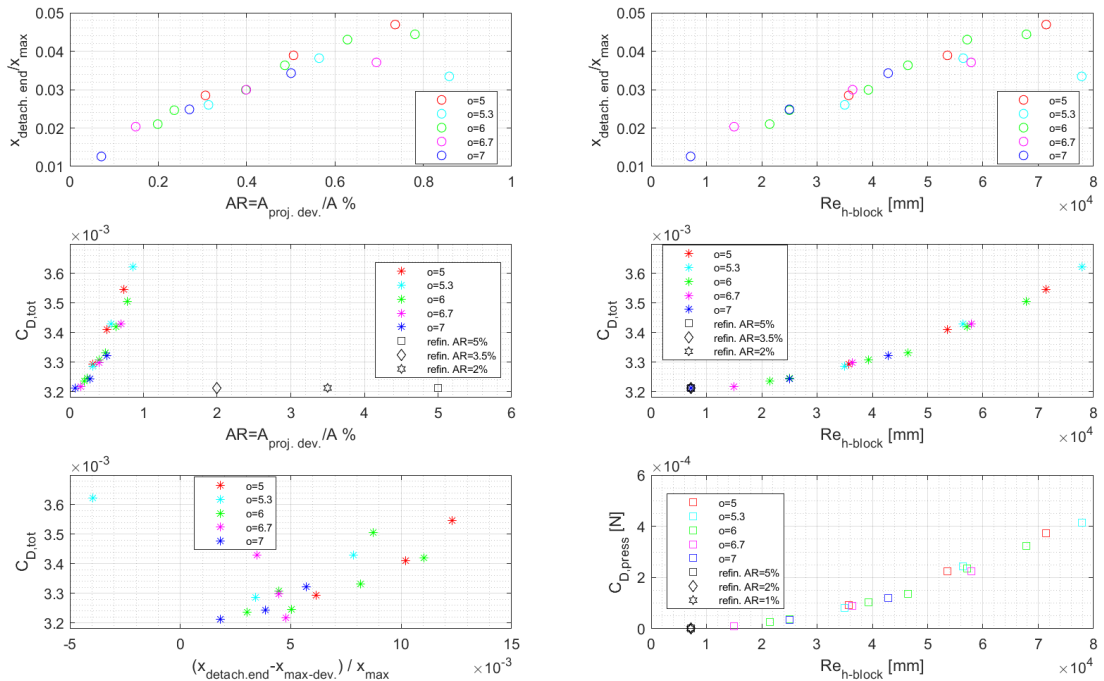
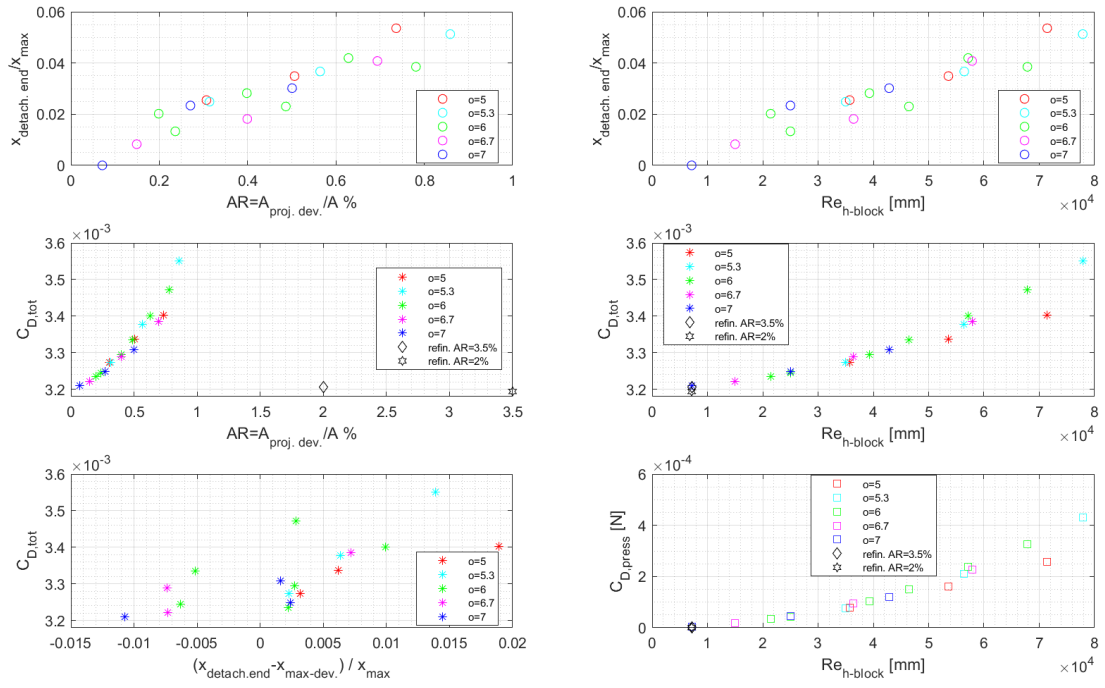


Figure 46: cumulative plot for the single pimple case



**Figure 47:** cumulative plot for the single dimple case

where

$$Re_{h-block} = \frac{\rho v h_{block}}{\mu} \quad h_{block} = diameter/2 - offset \quad (9)$$

$$AR = area - ratio = \frac{A_{projected,device}}{A_{flat-plate}} \quad C_{D,i} = \frac{D_i}{0.5\rho v^2 S} \quad (10)$$

$$(11)$$

To see what component of drag is varying more changing device configurations, a drag decomposition was made on the best and worst cases of the two problems, dividing the plate in zones as follows

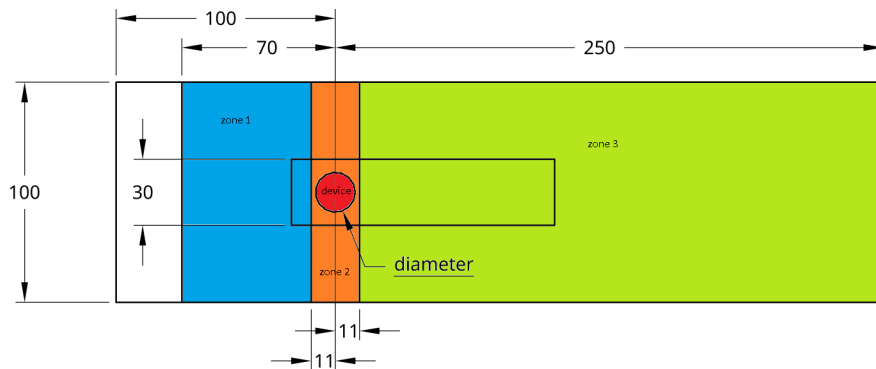


**Figure 48**

The drag was then computed on each zone: in the plane zones the only non-zero drag component was the viscous one, as there's no projected area in the direction of the flux, while on the devices the drag was decomposed in viscous and pressure-drag.

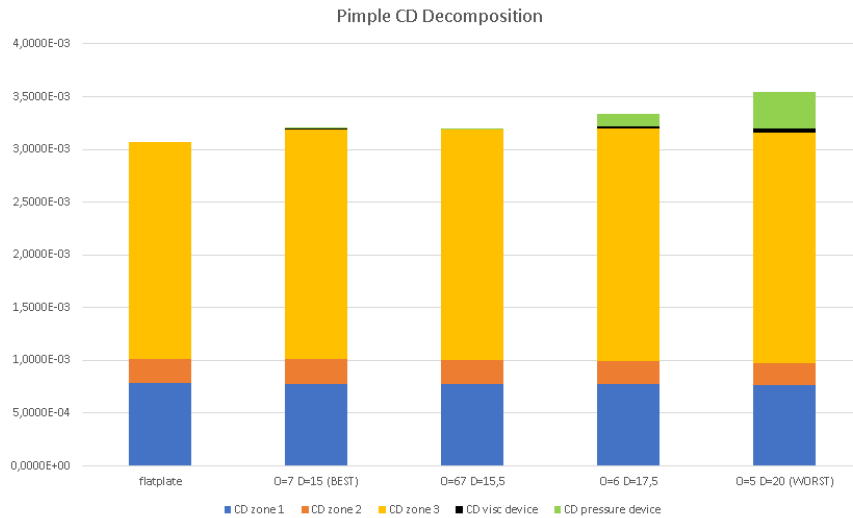


**Figure 49:** *single pimple: drag decomposition, the drag forces were made non-dimensional as in eq. 11. The flat-plate bar was made using the same geometry and mesh parameters as in the cases with pimple/dimple. Of course in that case there's no pressure drag*

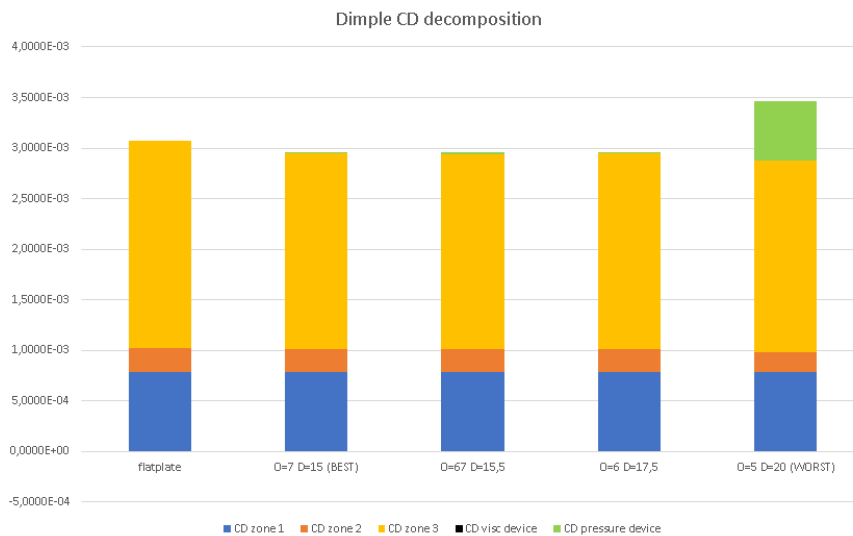


**Figure 50:** *single dimple: drag decomposition, the drag forces were made non-dimensional as in eq. 11. The flat-plate bar was made using the same geometry and mesh parameters as in the cases with pimple/dimple. Of course in that case there's no pressure drag*

From these plots we can say that significant geometrical variations result mainly in a variation of the pressure drag, as the other drag components show very slight variations. Regarding the previous set of parameters, now it makes sense to monitor the behaviour of the pressure drag as function of the non-dimensional blockage height and try to get a response curve of this dependence. To be precise, another parameter could have had a similar importance: the AR, but, using some refinement points with extreme AR (black

dots in figure), it was demonstrated that their dominance is only very local, while those points are packed with the previous curves if the blockage height is used as a geometrical parameter. As there might be noise due to the unsteadiness and to the mesh, a good approximation could be obtained using a least-square fitting, that minimizes the Euclidean Norm of the error and does not necessarily pass through each point. Using the Van der Monde matrix and the Moon-Penrose pseudo-inverse, nearly any function could be suitable for the fitting: in this case the simplest approximation was a 2nd order polynomial curve:

$$V = MA \rightarrow \begin{bmatrix} C_{Dp,1} \\ C_{Dp,2} \\ C_{Dp,3} \\ \dots \end{bmatrix} = \begin{bmatrix} 1 & Re_{hblock,1} & Re_{hblock,1}^2 \\ 1 & Re_{hblock,2} & Re_{hblock,2}^2 \\ 1 & Re_{hblock,3} & Re_{hblock,3}^2 \\ \dots & \dots & \dots \end{bmatrix} \begin{bmatrix} a_0 \\ a_1 \\ a_2 \end{bmatrix} \quad (12)$$

The Euclidean Norm of the error between  $V_{modelled,i}$  and real  $V_i$  is minimized if

$$A = (M^T M)^{-1} M^T V \quad (13)$$

That gives the fitting coefficients  $a_0$ ,  $a_1$ ,  $a_2$ . The only caution that has to be taken into account is that the inverted matrices should not be close to singularity (i.e. determinant close to zero), otherwise the LU decomposition implemented in MatLab command "inv" will not work properly.

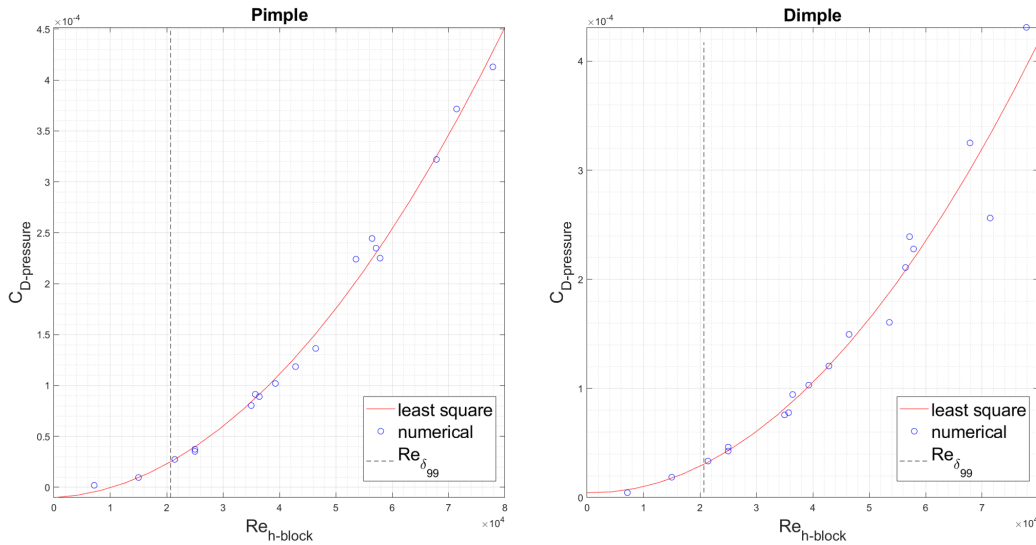


**Figure 51:** comparison of numerical data and least square fitting for pressure drag coefficient. The data were made non-dimensional as in the previous cases;  $Re_{\delta_{99}}$  is the Reynolds number based on the the boundary layer thickness:  $\delta_{99} = y \mid u(y) = 0.99u_{\infty}$

where the fitting curves are:

$$C_{D,p-pimple} = -1.0097 \cdot 10^{-5} + 2.7481 \cdot 10^{-10} Re_{h-block} + 6.8733 \cdot 10^{-14} Re_{h-block}^2 \quad (14)$$

$$C_{D,p-dimple} = 4.5005 \cdot 10^{-6} - 1.0591 \cdot 10^{-10} Re_{h-block} + 6.5812 \cdot 10^{-14} Re_{h-block}^2 \quad (15)$$

It is evident that, to get the minimum pressure drag (and so the minimum total drag with a single device, as previously demonstrated) a device with very small blockage height is

needed. It is interesting to point out that the fitting curve flattens under the boundary layer height, whose corresponding  $Re$  is plotted in the previous figures. Further plots in normalized coordinates will be present afterwards on this topic. The best examined case, that is a device with offset 7mm and diameter 15mm, will be taken as a basis for the 2-devices computations: this operation let us save a big number of computations and reduces the parameters of the future computations to only 2: the movement of the downstream device on the x-axis and that on the z-axis. This case is presented in the following section.

## 6 Part 3: 3D flat plate: pattern of 2 devices with 2D movement

### 6.1 Introduction

In this section the movement along two axes of a second device in the downstream zone of a first device is presented. Since we have first demonstrated that the key to reduce drag is to keep pressure-drag low, we will keep the "blockage-height" of the devices to the optimal solution found in the previous section. This corresponds, in our case, to a device of diameter 15mm with an offset of 7mm; in non dimensional units,  $Re_{h-block} = 7143$ . One could disagree with this statement, but it is necessary to consider that the optimal solution provided by the least-square method would correspond to a plate with no device in the case of pimple and with a device whose dimensions are very close to the ones reported in the case of dimple, as the least-square curve is nearly flat in the optimal region. For these reasons it is acceptable to consider the  $Re_{h-block} = 7143$  as the best case possible with a single device and start the following computations using this assumption.

Another important topic to consider in these computations is that, to get a proper resolution of the viscous effects downstream the devices, a much finer mesh will be required and a body of influence including the devices will necessarily have to go downstream until the pressure outlet, otherwise the numerical diffusion will disrupt the vortices and the viscous effects (that are dominant in this case) will not be predicted in a correct way. A problem regarding this topic is that a complete refinement of the whole downstream plate with a  $R_L \approx 5$  would cost at least 12 million cells, which is unaffordable for our computers. Then the boundary conditions do have an impact on the number of cells: a "slip-wall" BC as in the previous case would require or a very big domain or a moving-walls domain. In both cases, this would be, again, unaffordable. A solution to our computational limitations can be this one:

- use periodic BCs on left and right sides combined with a slip-wall on the top
- use 2 bodies of influence: one fixed on the upstream device and one movable, that follows the downstream device. This, combined with a proper reduction of the growth rates of the mesh, can reduce significantly the mesh size, leading to a mesh of  $1.5 \div 3$  million cells.

This mesh is at the limits of affordability for our computations.

Another problem is that we would need to calculate a response surface for each configuration: Pimple-Pimple (PP), Pimple-Dimple (PD), Dimple-Pimple (DP) and Dimple-Dimple (DD). The number of computations required for the purpose is too big for the given timetable, so some preliminary computations are set to capture if there is a con-

figuration that is more promising than others. To save on the number of cells, these computations are made with pimples/dimples "in-line" (so they are included in the same body of influence). The geometry and the mesh settings are presented below, while the setup is the same as in the previous section.

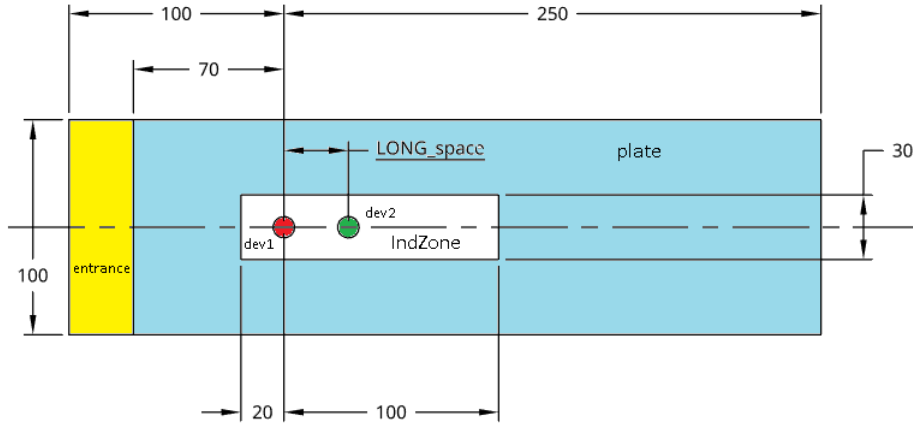


**Figure 52:** geometry sketch and zone names for the double-device preliminary computation

Mesh settings:

- mesh max size: 25mm
- body of influence: 0.8mm, growth rate 1.1 (the body of influence corresponds to the IndZone and is extruded for 15mm)
- face sizing plate: 3.5mm, behaviour: soft, growth rate 1.1
- face sizing IndZone and devices: 0.8mm, growth rate 1.1
- Inflation layers on the zones dev1, dev2, plate, IndZone, entrance: first layer height: 0.0025mm, 35 layers, growth rate 1.14.

These mesh-settings produce a  $y_{average}^+ < 1$  and a  $y_{max}^+ < 2$ . Skewness and Orthogonal quality are always in the prescribed limits. Below, the results of these preliminary computations are presented:

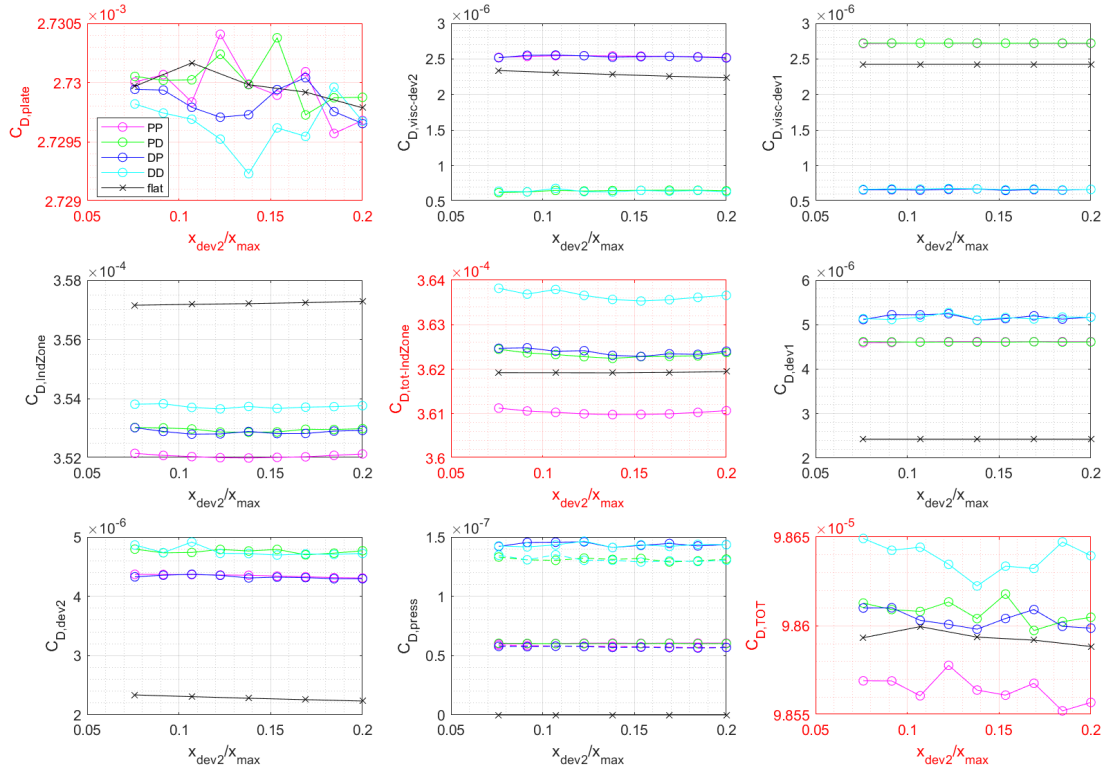


**Figure 53:** Results of PP,PD,DP,DD and flat plate cases decomposed for zones and for component of drag (when possible), the sum of the first two results in red is shown in the last chart in red. Drag coefficients are obtained by dividing the drag force for  $0.5\rho v^2 S$ : this generates very low values of these coefficients, but conserves the relation  $C_{D-tot} = \sum_i C_{D,i}$ . The cases with devices are compared with a flat plate that has the same zones as the cases with device, but the zone corresponding to the devices are the projection on the base plane of the devices (so they are flat).

These results suggest

- that the mesh is too coarse or the meshing algorithm is not perfect (in fact the flat plate total drag shows some oscillation, but it shouldn't: it is always the same flat plate with moving flat zones)
- the best cases is always the PP: it seems to be able to produce a drag inferior to that of the flat plate, while the other configurations are always above that limit.

For these reasons and to achieve a major numerical stability, the conclusive computations were concentrated on the PP case and the mesh was made using Fluent-Meshing, that has a finer algorithm which is able to generate poli-hexa meshes, which will allow faster and more accurate results. Unfortunately, Fluent meshing can't work in the DOE/RSM loop of Ansys Workbench because its scripts are generated and cancelled every time the project is updated, so the computations are to be generated and launched by hand and the response surface has to be generated using a proper hand-made script, too.

### 6.2 Geometry and mesh

The geometry adopted is different from the previous case because we want to optimize the number of cells and use periodic boundary conditions, as previously discussed

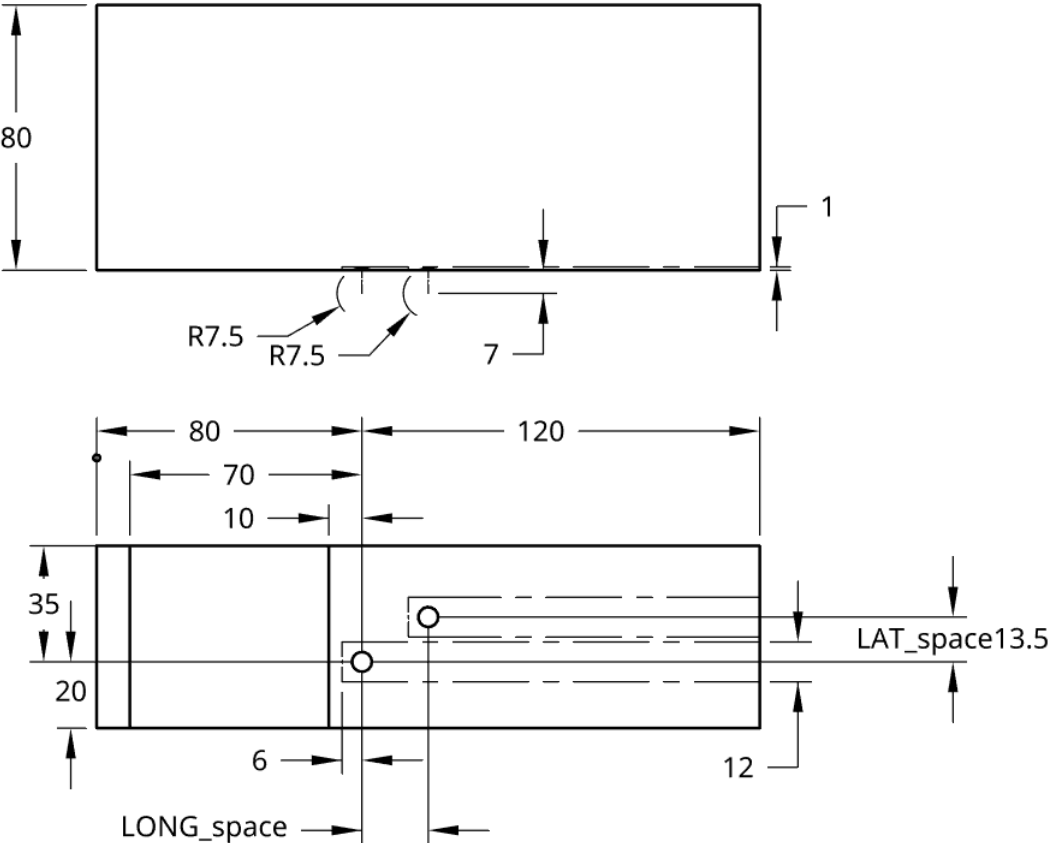


**Figure 54:** geometry sketch for the final double-pimple computation, dimensions are in [mm], underlined names are parameters. Bodies of influence are drawn in dash-dot line

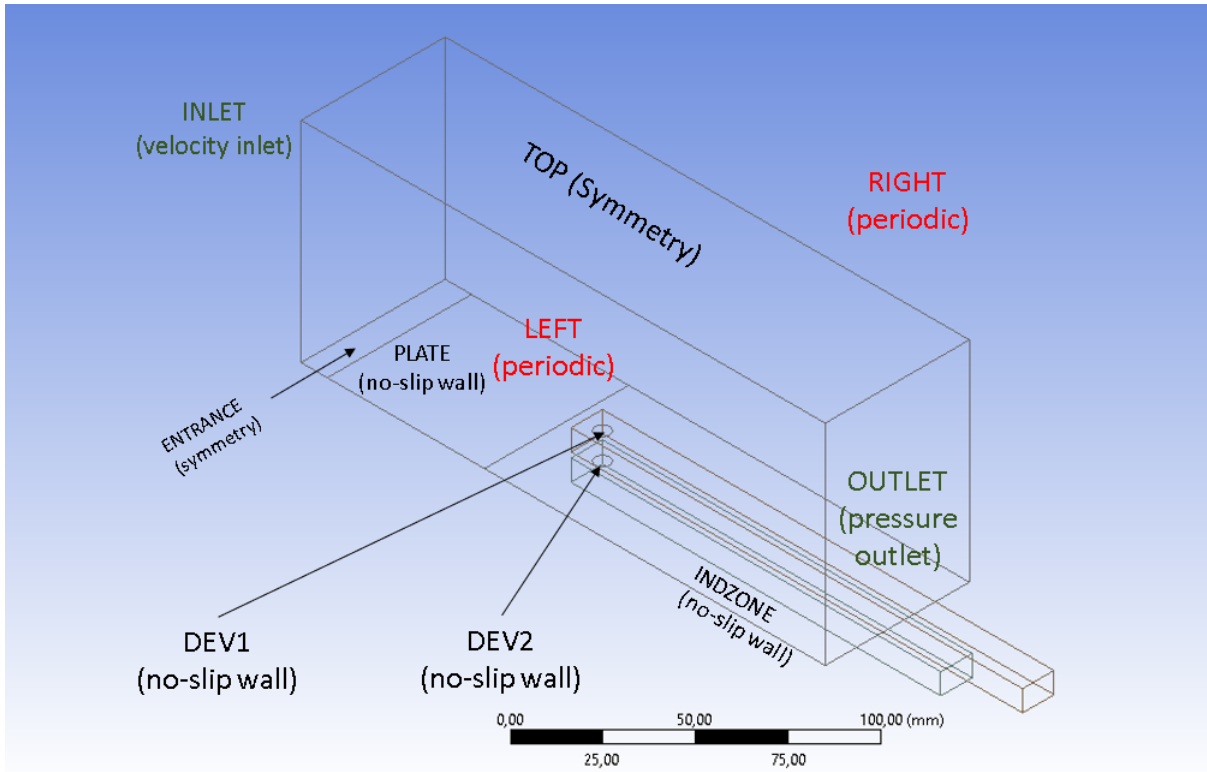


**Figure 55:** boundary conditions and zone names for the final double-dimple computation

The mesh was obtained using Fluent-Meshing with the following parameters:

- workflow: watertight geometry
- bodies of influence: target size 0.2mm, growth rate 1.15
- curvature on *dev1* and *dev2*: local min size 0.1mm, max 0.12mm; curvature normal angle 3°; growth rate 1.11
- face sizing on *IndZone*: target size 2.8mm, growth rate 1.12
- face sizing on *plate*: target size 3mm , growth rate 1.2
- face sizing on *left*, *right*, *inlet*, *outlet*, *top*: target size 20mm, growth rate 1.2
- prism layers on all bottom walls: "last-ratio" option with last layer  $2.3 \cdot 10^{-3}mm$ , 15 layers, ratio 0.272 (default).

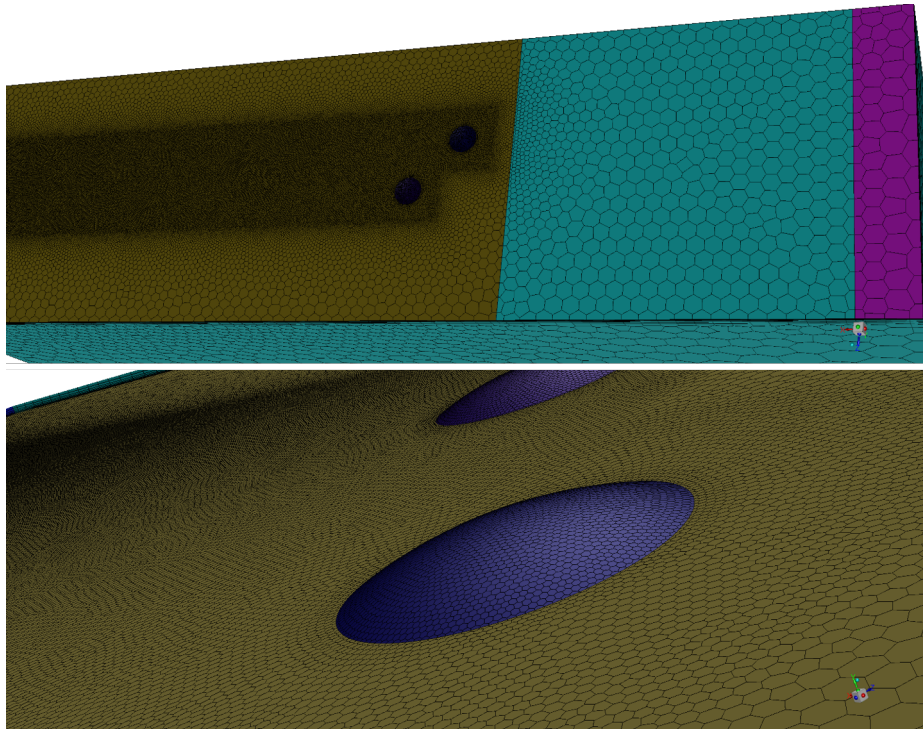


**Figure 56:** *surface mesh near and on the pimples. Curvature is well resolved with the given parameters.*

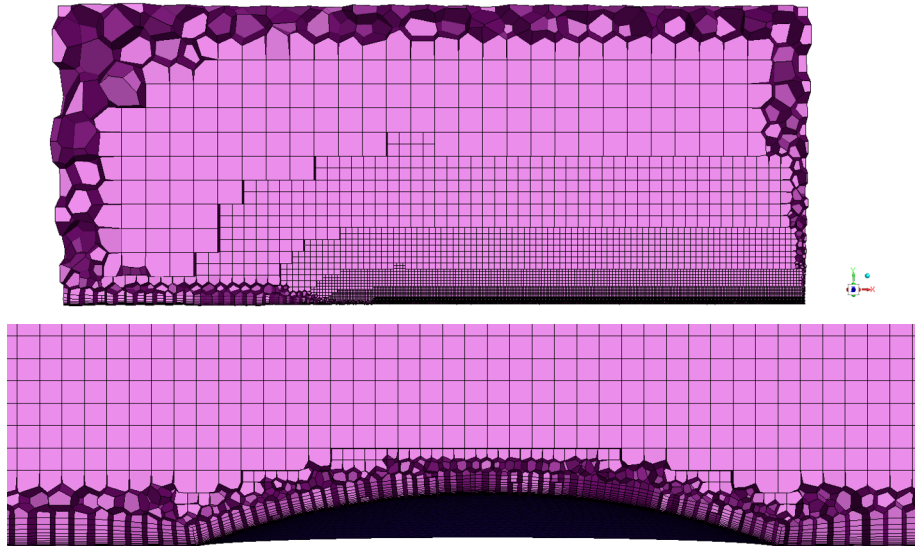


**Figure 57:** *interior of the mesh with a pimple in detail. The mesh is polyhedral near the walls and becomes hexahedral far from the walls, allowing a very high quality of the mesh: in no cases orthogonal quality is inferior to 0.2 and is generally higher*

## 6.3 Setup

The simulation is again steady, with the assumption of isothermal, Newtonian, fully turbulent, incompressible flow. These assumptions are reasonable as the flow has  $Ma < 0.3$  and  $Re_x = 10^6$  at the location of the first pimple, as in the previous computations. For these reasons we can assume a molecular viscosity of  $\mu = 3.43 \cdot 10^{-6}$ . The solver is pressure-based and "gravity" option is not enabled as its influence is negligible in aerodynamics. The turbulence model is the *SST*  $k - \omega$  with curvature correction and production limiter option enabled. Curvature correction is necessary as we want to resolve well the vortices in the wake of the devices and the horseshoe vortex starts with a zone where swirling is dominant. A more "physical" (because it doesn't contain the Boussinesq's Hypothesis like the *SST*  $k - \omega$  [7]) turbulence model like the *Reynolds Stress Transport* would be more appropriated, but that model is not easy to converge and is much heavier than the *SST*  $k - \omega$ , which is, however, capable of very good predictions even in swirling flows when the curvature correction is enabled. For this reason the *SST*  $k - \omega$  is the final choice. To get an acceptable computational cost and as we want to examine what happens in a fully-turbulent BL (that will be the case of the Ahmed body), the transition model was not enabled.

The boundary conditions are described in figure 55 and are essentially the same as in the previous computations; the only exception is the periodic boundary condition on the lateral walls: to impose this kind of BCs there are two ways in Fluent:

1. having a mesh with perfectly equal correspondent faces on the periodic interfaces and use the TUI commands to make them periodic. This will automatically associate the corresponding faces to get the periodicity BC.
2. having a mesh with similar (but not equal) faces on the periodic interfaces, set the zones as "interface" and use the following command in the TUI: `define > mesh - interfaces > make - periodic`, then choose the right face as "periodic" and the left one as "shadow"; the distance between the faces will be automatically calculated. This method allows the imposition of a periodic BC on meshes that don't have equal faces, but this interpolation operation will -of course- generate a little error. To quantify this error, the mass-imbalance was computed for each calculation, confirming that in this case this error is very similar, as order of magnitude, to the mass-imbalance between inlet and outlet. Both are negligible. However, as mass is not the only transported quantity, the distance between the pimples and the periodic interfaces was chosen in order to avoid high pressure gradients at the interfaces (in fact the pressure gradients are nearly extinguished at  $\approx 15mm$  from the center of the pimple) and so, in some ways, limit eventual interpolation errors.

Some minor changes to the previous setup are:

- set stricter convergence conditions on continuity:  $10^{-6}$ : this is, in fact, a reasonable limit generally reached in any of the present cases and may be helpful when going to the adjoint solver, which requires very well converged solutions.
- use autosave option to retain data in case of problems. This option is needed in this case as cases run for a much longer time than in the previous cases (1-2 hours).
- enable the data sampling for steady statistics, which will be useful for further post-

processing, that is part of the main project, but is not directly presented here.

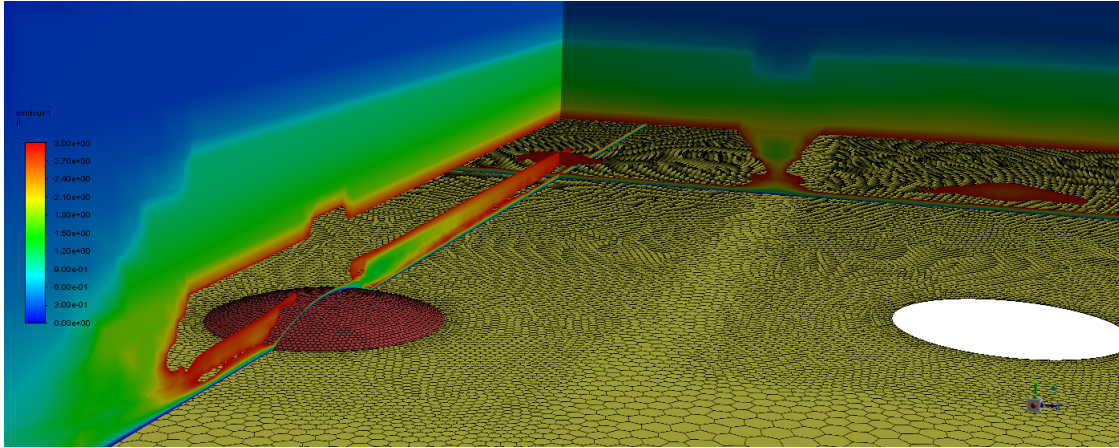


**Figure 58:**  $R_L$  criterion contours limited to a scale of  $0 \div 3$  to show the zones where RANS models may fail to capture the correct behaviour of the integral scales: in our case the horseshoe vortices are well resolved but the mesh would require refinement just after the pimple. However, this was the best mesh we could afford with the given computational resources

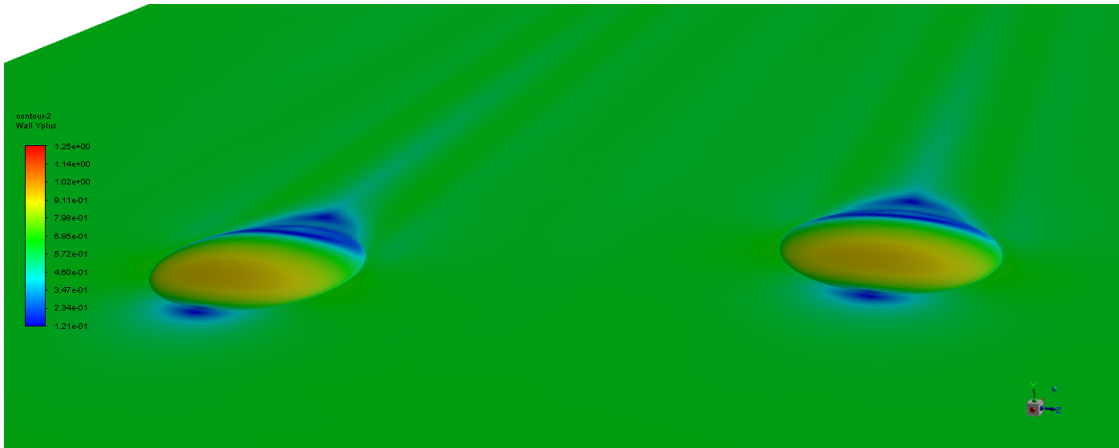


**Figure 59:**  $y^+$  contours on IndZone and the devices: the boundary layer is everywhere correctly resolved at least for what regards the first cell height: the maximum  $y^+$  never enters the buffer layer and the minimum  $y^+$  is never lower than 0.1 (issue that could generate numerical oscillations)

## 6.4 Optimization

Forced by the fact that periodic BCs and the use of Fluent Meshing do not give us the opportunity to implement the optimization loop directly on Ansys Workbench, the Design of Experiment (DOE) will be made using a central composite technique with 16 points, equally spaced longitudinally and laterally (the chosen step is 5mm, that is about the "flux diameter", 5.3852mm), that is more expensive than a Latin Hypercube, for example, but may be helpful to see the dependence from the single coordinates on the plane.

Using a least square fitting with a 4th order polynomial of the DOE points, it was possible to find a trend of how the drag varies in function of pimples positioning: in fact, even if the drag doesn't change a lot (in the cases of interaction between the horseshoe vortex of

the leading pimple and the body of the second pimple the drag increases of around the 0.2%) it can be found that it has its lowest value when the vortices of the two pimples don't interact and when they are positioned nearly on the same line and not downstream-staggered (figure 60).

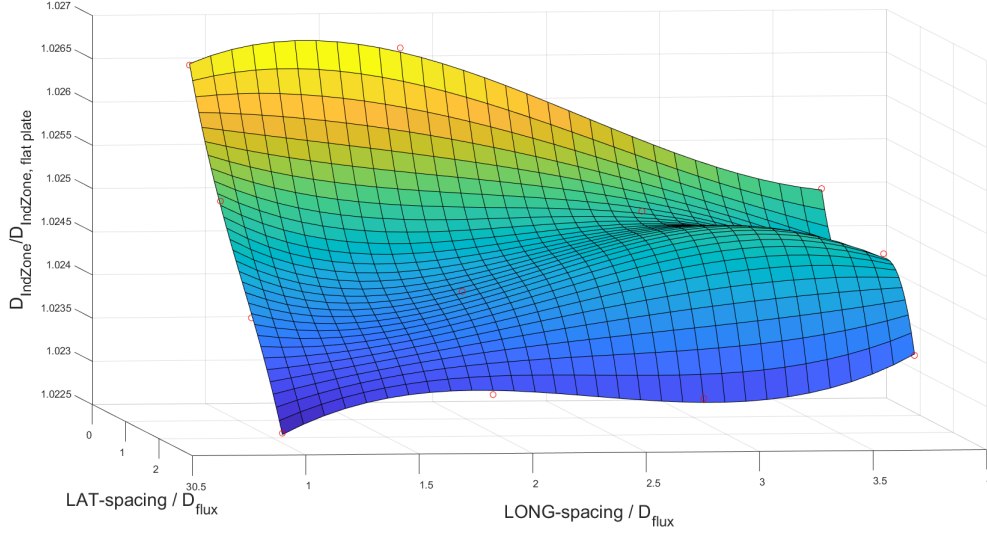


**Figure 60:** Response surface for the case of double pimples: drag on the IndZone is normalized with drag of the flat-plate ( $D_{indzone,flat} = 0.02038N$ , or  $C_{D-IndZone,flat} = 0.002$ ) on the same zone and is plotted against the relative positioning of the two pimples, normalized with the "flux diameter" (the diameter of the projection of the pimple on the base plate, which is, in this case, 5.3852mm). Red points are the numerical Fluent simulations. The response surface has a  $R = \sqrt{1 - \frac{\sum_{i=1}^N (y_i - \hat{y}_i)^2}{\sum_{i=1}^N (y_i - \bar{y})^2}} = 0.9972$  and  $R_{adjusted} = \sqrt{1 - \frac{\sum_{i=1}^N (y_i - \hat{y}_i)^2}{\sum_{i=1}^N (y_i - \bar{y})^2} \frac{N-1}{N-m}} = 0.9965$ . Where  $\bar{y}$  is the mean,  $\hat{y}_i$  is a predicted point value and  $y_i$  the correspondent measured value,  $N$ =number of experiments. The provided values of  $R$  show that there is a really good agreement between DOE points and least square surface

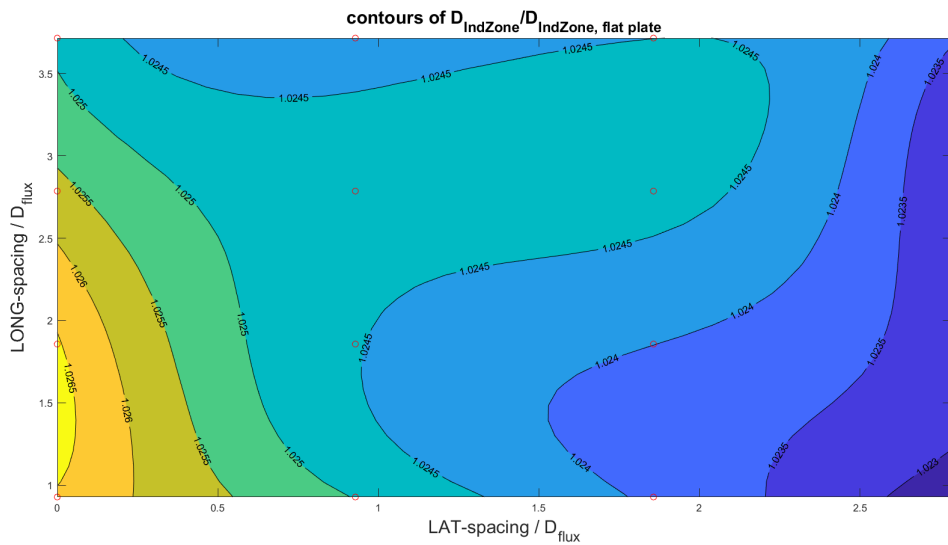


**Figure 61:** contour plot of the response surface for the case of double pimples. Parameters are the same as in the previous figure. Red points are the numerical Fluent simulations

The response surface shows that the best case occurs when the pimples do not have a significant interference with their wakes: the response surface in this case may be helpful to understand which parameter is more important, but fails to predict a global minimum, as we have found that the minimum is one of the DOE points and stands near the DOE limits. However, this surface suggests that when two pimples are very near and in-line, their horseshoe vortices have a positive interference (they try to enforce one another) and this generates a flatter velocity profile downstream, increasing the drag. On the other hand, when interaction is limited by staggering the two pimples, the drag shows a rapid and monotonic decrease if the pimples are longitudinally "near", while this behaviour is not monotonic if they are longitudinally more distant and there may be local minima, where a direct optimization would fail to capture the overall behaviour (the global minimum). It is important to notice that lateral spacing governs how the coherent structures interact (because those structures are elongated in the x-direction), while longitudinal spacing governs diffusion and makes the second pimple find zones of increased or decreased x-wall shear stress. In fact we have shown that the  $\tau_{wall,x}$  shows non asymptotic behaviours downstream the pimple, so if a second pimple is positioned very near to the first, higher wall-shear will be produced, while if it is positioned more downstream, it will find smaller  $\tau_{wall,x}$  values. Diffusion is present as the vortices become larger but less intense going downstream and this causes a variation in the zones of  $\tau_{wall,x}$ . We have, in fact, shown that those zones are very strictly related to the position with respect to the vortices centerlines.

In any case, the new analysis, which is much stronger than the previous "preliminary" computations, show that the drag produced by the pimples surface is always higher than that produced by the flat plate, that is partially in contrast with the preliminary computations. For this reason, deeper studies will be made using also the other configurations (DP,PD,DD). However, these computations are not presented in this paper.

One major reason to focus on the PP case, however, lies in the fact that pimples are -on the contrary of dimples- devices that help the boundary layer to stay attached to diffusers. Some of our preliminary computations have demonstrated this fact, which is also very intuitive (horseshoe vortices are very strong compared to dimple's cyclones, pimples change the diffuser angle "smoothing" the passage between channel and diffuser), so it does make sense to study first the PP case and then, eventually, check all the other combinations.

The contributions of the different "components" of the geometry to drag were computed to find out what component varies mostly from the two cases: the results of the comparison can be found in tab. 4.

	$C_{Dv,dev1}$	$C_{Dv,dev2}$	$C_{Dp,dev1}$	$C_{Dp,dev2}$	$C_{D,dev1}$	$C_{D,dev2}$	$C_{D,IZ-tot}$
best	7,78E-06	7,73E-06	6,28E-06	6,09E-06	1,41E-05	1,38E-05	2,03E-03
worst	7,68E-06	7,43E-06	5,31E-06	6,99E-06	1,30E-05	1,44E-05	2,04E-03
var %	+1,40%	+4,08%	+18,17%	-12,89%	+8,26%	-4,15%	-0,38%

**Table 4:** Drag decomposition for the best and worst case: percentage variations are computed as  $var\% = \frac{x_{best}-x_{worst}}{x_{worst}}$ , the nomenclature used is the following: IZ= IndZone, dev1,2= device 1,2 (1st, 2nd pimple), v=viscous, p=pressure. Best and worst cases have respectively 15mm and 0 mm lateral spacing and 0mm and 10mm longitudinal spacing. Drag coefficients are obtained as described previously.

From this decomposition it is evident that the combined effect of the horseshoe vortices and their interaction are responsible for the variations of drag on the plate: the drag coefficient variations on the two devices are in fact opposed to the variations of the drag on the IndZone: viscous drag on the devices show an increase from the worst to the best case, while pressure drag shows an increase on the first pimple and a decrease on the second (and this is reasonable: in incompressible regime upstream flow is conditioned also by devices placed downstream; then the second pimple, in the in-line configuration, is "hidden" by the first pimple, while it is not when they are staggered). The two variations generate an improvement on the second pimple and a deterioration on the first one, but despite these local variations, there is a global improvement in the downstream zone that make the global drag decrease.

## 6.5 Results

In this section the hypothesis made in the previous section are supported using some post-processing: first of all it is interesting to see a combined map of velocity and x-wall Shear stress. The velocity is plotted on a Q-criterion iso-surface to highlight the vortices: as in the preliminary computations, pimples generate a flow pattern that divides the plate into stripes of alternate improvement and deterioration of viscous drag. The lines that divide these zones are the axes of the vortices: where air is pulled up, there drag diminishes, where air is pushed down, there drag increases. It is interesting to notice that the in-line pattern generates very strong vortices (it is quite impossible to say if the two horseshoe vortices come together into a single filament or if the two remain separated but one stands onto o near to the other) that certainly pushes down air downstream the pimples -increasing wall shear stress- but does not, on the contrary, increase also the "pull-up" effect, so producing a negative effect.

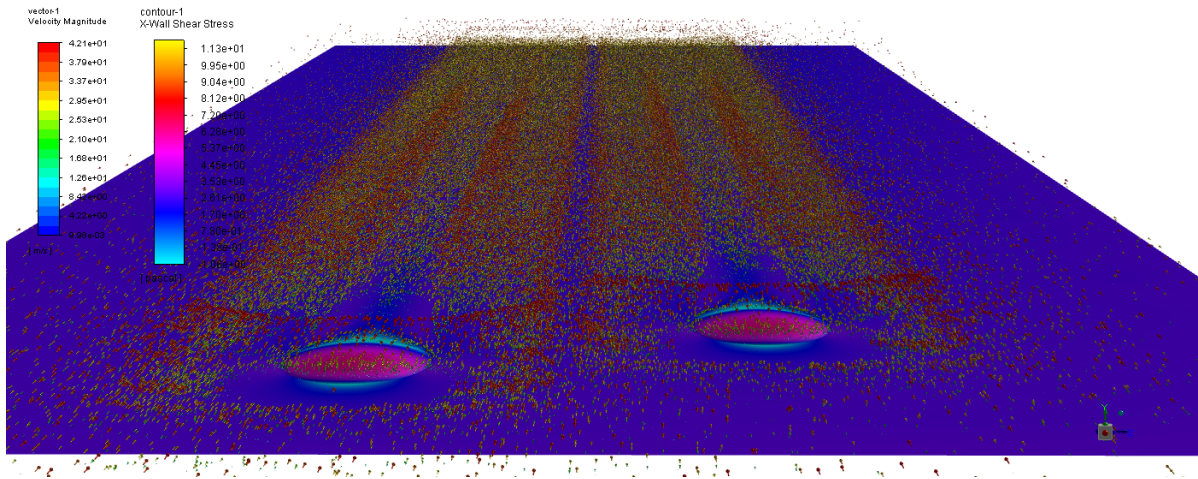


**Figure 62:** combined plot of X- wall shear stress on the IndZone and velocity vectors on a iso-surface of Q-criterion: it is the best case found. The vortices of the two devices do not interact or their interaction is negligible

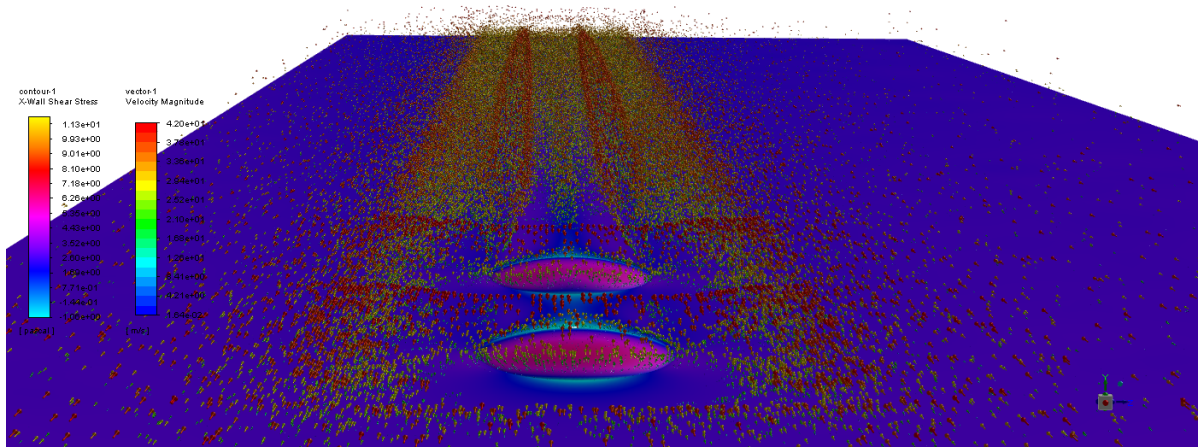


**Figure 63:** combined plot of X- wall shear stress on the IndZone and velocity vectors on a iso-surface of Q-criterion: worst case found. Here the vortices of the two devices do interact, forming a much stronger vortex

To advocate the in-line configuration, that is the worst in our case, we may imagine that having stronger vortices may generate an improvement where BL detachment could be repaired by a strong injection of momentum into the BL using vortices like those, so when we will study the pimped-diffuser, we will need to take this into account.

Then it may be interesting to plot the non-dimensional velocity  $u^+$  against the non-dimensional distance from the wall,  $y^+$ , to see how the pimple interacts with the boundary layer. Taking the wall shear stress value at the location of the center of the 1st pimple, the corresponding  $y^+$  is 297.07, so the pimple trepasses all 3 layers but it isn't high enough to enter the fully-developed flow zone, as it can be seen in fig 65.

Then, a comparison between the non-dimensional velocity plots at different locations near the pimple may be interesting:

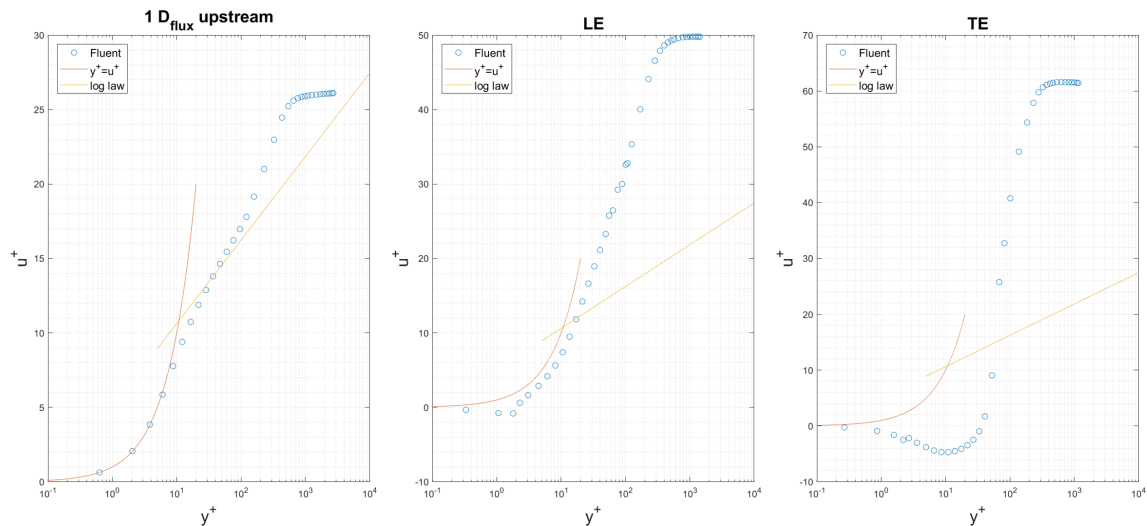


**Figure 64:**  $u^+ = u/U_\tau$  against  $y^+ = yU_\tau/\nu$  plot, where  $U_\tau = \sqrt{\frac{\tau_w}{\rho}}$ . The plots are referenced to 3 lines: one that is 5.3852mm upstream the leading edge (LE) of the pimple center, one on the leading edge and the pimple and the last on its trailing edge (TE)).

It is quite clear that in the first plot, that is taken  $1 D_{flux}$  upstream of the center of the pimple, the flux is quite undisturbed and in fact there is very good agreement between theoretical profiles and Fluent data. The log-law zone in the Fluent profile is quite strict, but we managed to get at least 4 points in the log-law zone and we have resolved correctly the viscous sublayer, so we can conclude that the chosen expansion ratio for the prism layers is correct.

In the other two figures the same plot is proposed where there are two significant variations in geometry: the leading (accelerating flux) and the trailing edge (detachment). In the central figure the boundary layer is detached (negative  $u^+$ ) very locally but the flux seems then to follow the law  $u^+ = y^+$  and the log-law layer seems disappeared. In the third figure the BL is completely detached. The following figures are made for comparison at the same locations as in the previous figure, but on a flat plate: of course these figures do show a complete agreement with theoretical profiles for each location.

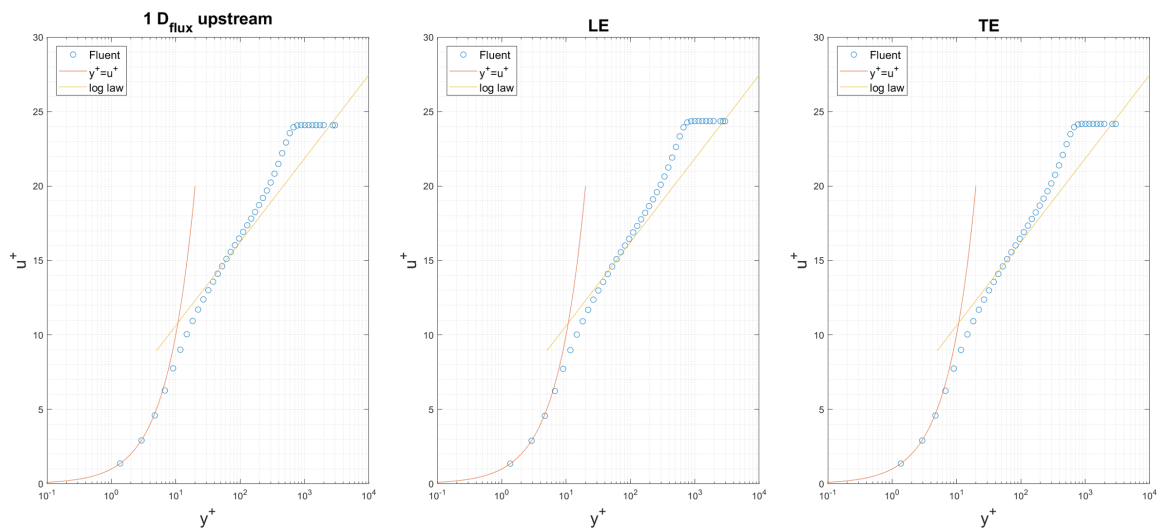


**Figure 65:** Reference plots of the non-dimensional velocity evaluated at the same measurement stations as in the previous case, but for the flat plate case

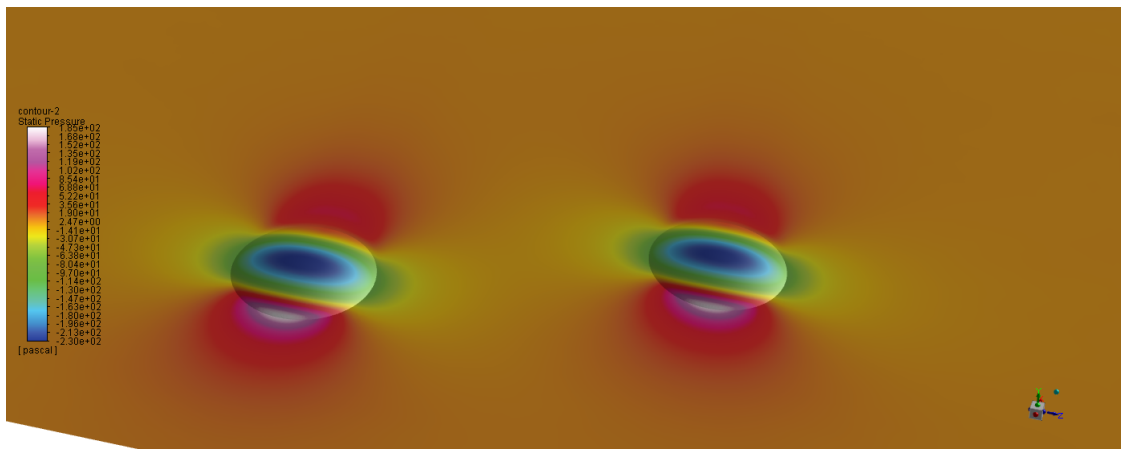


**Figure 66:** pressure contours for the best case: the interaction between the pimples are only due to the pressure field

## 7 Part 4: 3D shape sensitivity map using Fluent adjoint solver

In the previous section we have demonstrated that an optimal point in terms of drag is reached when the pimples do not interact. This result is not new to literature, even if not applied on a flat plate, and it can be found in the 2011 24h-Le Mans racing car of the team Oak Racing [8].



**Figure 67:** Oak Tree team 2011 racing car, rear wing: notice the single row of pimples

For this reason, it makes no sense to examine two pimples at one time using the adjoint solver to get the shape-sensitivity maps: the same result can be obtained using a single-pimple case, that is much more affordable.

### 7.1 Geometry, mesh and setup

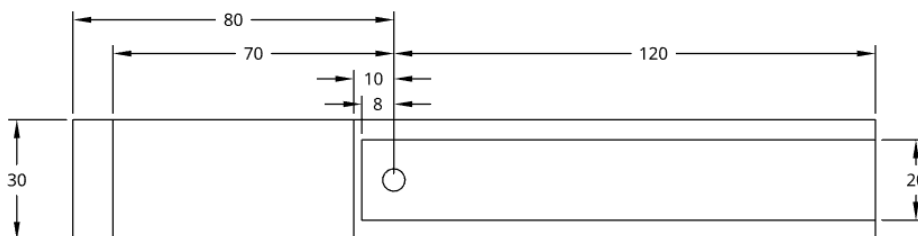


**Figure 68:** geometry used for the adjoint computation

The geometry and boundary conditions do not differ substantially from the previous case: the only difference is that the lateral periodic interfaces are distant 15mm from the centerline and the body of influence is a little bit larger but has cells sized 0.4mm

instead of 0.2mm, to save on cells. The mesh has  $\approx 750000$  poli-hexa cells and minimum orthogonal quality 0.34 .

## 7.2 Adjoint Setup

To start the adjoint calculation, a converged direct solution is needed first: this was provided using the same setup as in the previous case. This case has the same very smooth convergence of the previous case and is initialised with a converged solution to speed up the whole process.

After this point, in the "design" tab, an observable for the drag computed on the *IndZone* is created and set to "minimize". The adjoint solution methods are the default ones:

- method: Green-Gauss node based
- pressure: standard
- momentum: first order upwind

These parameters may be certainly improved, but it is essential to get a very well converged adjoint solution, so we will use these parameters, that are easier to converge. Note that it is not required to have a second order accuracy as in the case of the direct solution. The monitors are set as default except for the continuity, whose value is changed to  $10^{-6}$ , that is more appropriate, as we want very well converged solutions. The solver parameters and stabilization techniques are described in [4] and the workflow described there is followed strictly to get the solution converged as fast as possible. In fact this is not automatically reached by the Fluent Auto-Adjust, but requires some manual changes. The objective is reached in about 200 iterations, so the cost of the adjoint solution is of the same order of the direct one.

## 7.3 Results

To examine the results of the adjoint solution, a shape sensitivity vector plot is generated on the device: this map shows where one should "pull in" or "push out" the geometry to get a minimization of the drag on the *IndZone* (that corresponds to the pimple and its wake, or the projection of the body of influence).

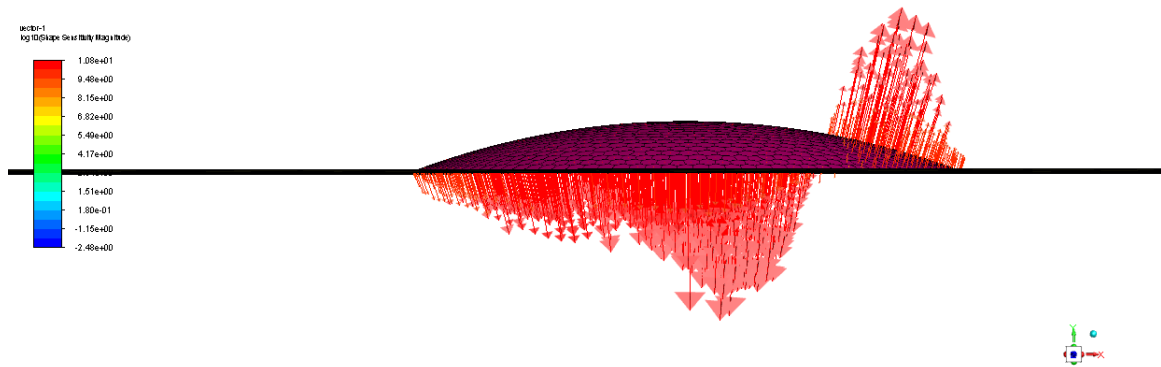


**Figure 69:** *shape sensitivity magnitude vector plot, colors have a log scale*

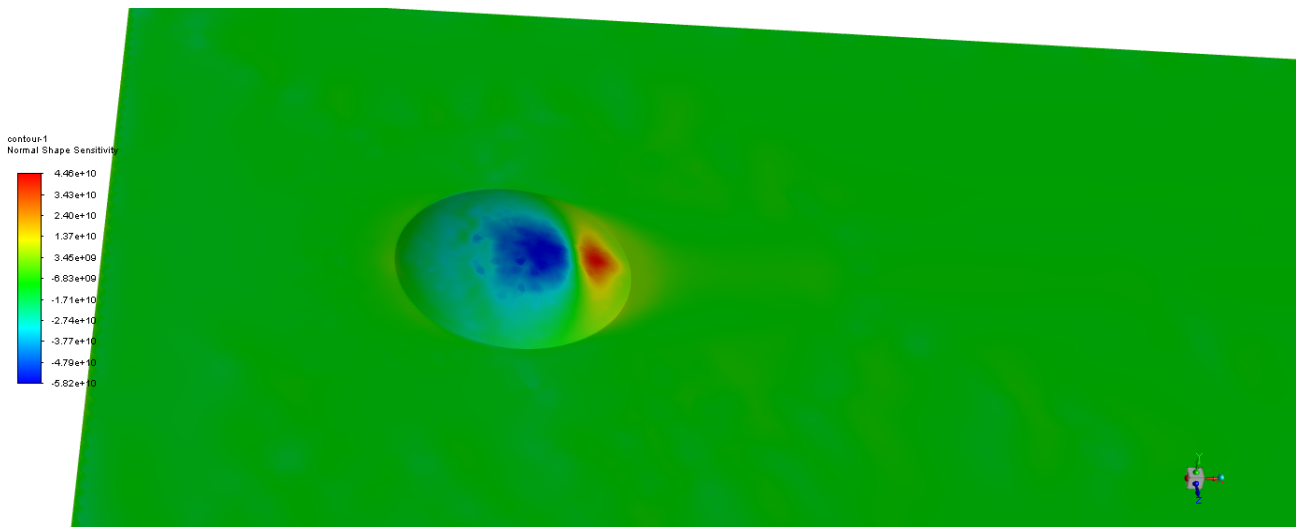


**Figure 70:** *normal shape sensitivity contour plot*

As expected (also from 2D computations) the pimple should be flattened and made "like a water drop" to minimize drag.

The great advantage of using the adjoint to compute the shape sensitivity is that it has a computational cost of one calculation, while if one had to compute the same map/gradient using a direct approach, the cost would increase as the number of points on the geometry increase.

## 8 Conclusions

Here a summary of the main results that we have found so far is presented:

- pressure drag must be taken into account making flatter devices that do not alter the flat plate conditions excessively. The blockage height is the dominant parameter when dealing with pressure drag and 2D and 3D agree on this;

- single pimple generate a horseshoe vortex that is steady, very stable and divides the downstream zone into stripes where viscous drag is alternatively improved or worsened; single dimple devices generate cyclone-like vortices or more complicated patterns that show more unsteadiness;
- the double-device case, under the (reasonable) assumption that the case PP is the best among the other configurations, turns out to be optimal when there is a single row of pimples. This -of course- stands for a flat-plate base geometry, but should be validated in case of a diffuser. 2D and 3D computations confirm this point;
- the optimal shape of a single pimple is confirmed both in 2D and 3D adjoint calculations: to reduce the drag the pimple should be "flattened and rear-slanted". If more adjoint iterations were run, the result would be probably brought to the extreme of recreating a flat plate;
- interactions between wakes or pressure gradients should be avoided as much as possible because, at least on a flat plate, they don't guarantee any advantage, causing a higher viscous drag behind the pimples.

## References

- [1] Intermittency transition model, ansys fluent 2020r1, help system, ansys fluent theory guide, ansys, inc. [https://ansyshelp.ansys.com/account/secured?returnurl=/Views/Secured/corp/v201/en/flu\\_th/flu\\_th\\_sec\\_turb\\_intermittency\\_over.html](https://ansyshelp.ansys.com/account/secured?returnurl=/Views/Secured/corp/v201/en/flu_th/flu_th_sec_turb_intermittency_over.html), 2020. Accessed: July 2020.
- [2] Curvature correction for the spalart-allmaras and two-equation models, ansys fluent 2020r1, help system, ansys fluent theory guide, ansys, inc. [https://ansyshelp.ansys.com/account/secured?returnurl=/Views/Secured/corp/v201/en/flu\\_th/flu\\_th\\_sec\\_curv\\_corr.html](https://ansyshelp.ansys.com/account/secured?returnurl=/Views/Secured/corp/v201/en/flu_th/flu_th_sec_curv_corr.html), 2020. Accessed: July 2020.
- [3] Model considerations for using adjoint solver, ansys fluent 2020r1, help system, ansys fluent theory guide, ansys, inc. [https://ansyshelp.ansys.com/account/secured?returnurl=/Views/Secured/corp/v201/en/flu\\_ug/flu\\_adj\\_sec\\_adjoint\\_usage\\_scope.html](https://ansyshelp.ansys.com/account/secured?returnurl=/Views/Secured/corp/v201/en/flu_ug/flu_adj_sec_adjoint_usage_scope.html), 2020. Accessed: July 2020.
- [4] P. Herberich O. Zühlke, C. Hill. Ansys fluent adjoint solver best practice guide. *Ansys Inc.*, 2015.
- [5] B. W. van Oudheusden F. F. J. Schrijer M. van Nesselrooij, L. L. M. Veldhuis. Drag reduction by means of dimpled surfaces in turbulent boundary layers. *Exp Fluids* 57:142, 2016.
- [6] H. Schlichting. Boundary layer theory, 7th edition. 1979.
- [7] Boussinesq approach vs. reynolds stress transport models, ansys fluent theory guide. <https://www.afs.enea.it/project/neptunius/docs/fluent/html/th/node47.htm>, Accessed: July 2020.
- [8] Racecar engineering: Can dimpled aerodynamic surfaces reduce drag? <https://www.racecar-engineering.com/articles/technology/can-dimpled-aerodynamic-surfaces-reduce-drag/>, Accessed: July 2020.